Supplementary Information

Hot Carrier Perovskites Solar Cell with Efficiency Exceeding 27% Enabled by Ultrafast Hot Hole Transfer with Phthalocyanines Derivatives

Shaokuan Gong[1]†, Geping Qu[2, 3]†, Ying Qiao[2]†, Yifan Wen[1], Yuling Huang[1], Siyuan Cai[2], Letian Zhang[2], Kui Jiang[4], Shang Liu[1], Meng Lin[1], Matthew C. Beard[5], Zong-Xiang Xu[2]*, Xihan Chen[1]*

[1] *Shenzhen Key Laboratory of Intelligent Robotics and Flexible Manufacturing Systems, SUSTech Energy Institute for Carbon Neutrality, Department of Mechanical and Energy Engineering, Southern University of Science and Technology, Shenzhen, Guangdong 518055, China.*

[2] *Department of Chemistry, Southern University of Science and Technology, Shenzhen, Guangdong 518055, China.*

[3] *School of Chemistry and Chemical Engineering, Harbin Institute of Technology, Harbin, 150001, China.*

[4] *Department of Materials Science and Engineering, City University of Hong Kong, Kowloon, 999077, Hong Kong*

[5] *National Renewable Energy Laboratory, Golden, CO, 80401, United States.*

**Corresponding author. Email: xuzx@sustech.edu.cn; chenxh@sustech.edu.cn*

†*These authors contributed equally to this work.*

Table of Contents

1. Supplementary Notes- Materials, Method and Modelling details

1.1 Materials

Unless specified otherwise, all materials were used as received. The materials used in the experiments included: cesium iodide (CsI; 99.999%, Sigma-Aldrich), Rubidium iodide (RbI; 99.9%, Sigma-Aldrich), methylammonium iodide (MAI; 99.5%, Xi'an Polymer Light Technology Corp.), formamidinium iodide (FAI; 99.5%, Xi'an Polymer Light Technology Corp.), dodecylamine hydroiodide (DDAI; 99.5%, Xi'an Polymer Light Technology Corp.), 2-phenylethanamine hydroiodide (PEAI; 99.5%, Xi'an Polymer Light Technology Corp.), polymethyl methacrylate (PMMA; 99%; BIDE), Lead iodide (PbI_2; 99.99%, Xi'an Polymer Light Technology Corp.), Methylammonium chloride (MACl; 99.99%, Xi'an Polymer Light Technology Corp.), Potassium hexafluorophosphate (KPF_6; 99.99%, Sigma-Aldrich), Ammonium chloride (NH_4Cl; 99.5%, Sigma-Aldrich), bis(trifluoromethane)sulfonimide lithium salt (LiTFSI; 99%, Xi'an Polymer Light Technology Corp.), cobalt(III) tris(bis(trifluoromethylsulfonyl)imide) (FK209; 99%, Xi'an Polymer Light Technology Corp.), Spiro-OMeTAD (99.8%, Xi'an Polymer Light Technology Corp.), deionized water (H_2O; Alfa Aesar), Tin(II) chloride dihydrate ($SnCl_2 \cdot 2H_2O$; 98%, Alfa Aesar), N,N-dimethylformamide (DMF; 99.8%, Sigma-Aldrich), dimethyl sulfoxide (DMSO; 99.9%, Sigma-Aldrich), ethanol (99.5%; Sigma-Aldrich), isopropanol (IPA; 99.5%; Sigma-Aldrich), chlorobenzene (CB; 99.8%; Sigma-Aldrich), 1,2-dichlorobenzene (99%, Sigma-Aldrich), acetone (99.8%; MERCK), 4-tert-butylpyridine (tBP; Sigma-Aldrich).

1.2 Instruments

NMR spectra were recorded on a Bruker AVANCE III 400M, and the chemical shifts were referenced internally using the residual solvent resonances. Mass spectra (MS) were recorded using a Voyager Elite MALDI-TOF mass spectrometer. Elemental analysis was performed using a Vario MICRO analyzer. The UV–vis spectra were recorded using a PerkinElmer Lambda750S spectrophotometer. The morphology of the prepared samples was also analysed using scanning electron microscopy (SEM, ZEISS_MERLIN). The contact angle measurements of the perovskites were performed using a drop shape analyzer (DSA 25S, KRUSS).

1.3 Synthesis of phthalocyanine compounds

Unless specified otherwise, all materials were used as received. Acetone was purchased from YONGHUA CHEMICAL CO., LTD. Other organic solvents and $CuCl_2$ were purchased from

Adamas-beta. 1-Butanethiol, 3,6-dihydroxyphthalonitrile, 4-methylbenzenesulfonyl chloride, and potassium carbonate were purchased from Bide pharmatech Ltd. 1,8-Diazabicyclo-[5,4,0]-undec-7-ene (DBU) was obtained from TCI (Shanghai, China). Copper (II) phthalocyanine (**Pristine Pc**, sublimed grade 99%) was purchased from Aldrich; Octal-methyl substituted Copper (II) Phthalocyanine (**Me_2Pc**) and methoxytriphenylamine-substituted copper phthalocyanine (**SMePc**) were synthesized and purified by reported procedure;[1,2] 1,4,8,11,15,18,22,25-octakis(butylthio)-substituted copper phthalocyanine (**SBuPc**) was synthesized and purified according to modified reported procedure. **(Scheme S1)**[3]

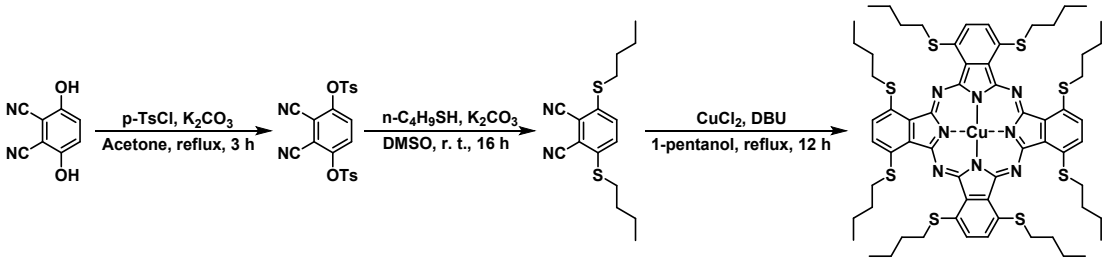

Scheme S1. Synthetic routes of SBuPc.

1.3.1 Synthesis of 3,6-bis(4'-methylphenylsulfonyloxy)phthalonitrile

4-Methylbenzenesulfonyl chloride (5.1 g, 27 mmol), 3,6-dihydroxyphthalonitrile (2.1 g, 13 mmol), potassium carbonate (6.9 g, 50 mmol), and acetone (30 mL) were added to an oven-dried 100 mL two-neck round-bottom flask. The mixture was heated to reflux for 3 h. After cooling, the mixture was poured into 100 mL deionized water and stirred for 30 min. The crude product was filtrated and rinsed with deionized water (4 × 30 mL) and acetone (3 × 2 mL) to afford colourless solid (5.0 g, 82%). ^{1}H NMR (400 MHz, $CDCl_3$) δ/ppm 7.83 (d, J = 8.4 Hz, 4H), 7.81 (s, 2H), 7.41 (d, J = 8.1 Hz, 4H), 2.50 (s, 6H). **(Supplementary Fig. S1)**

1.3.2 Synthesis of 3,6-bis(butylthio)phthalonitrile

An oven-dried 250 mL two-neck round-bottom flask was charged with 1-butanethiol (2.7 g, 30 mmol), potassium carbonate (5.5 g, 40 mmol), and 100 mL DMSO. The mixture was stirred for 30 min at room temperature. Then 3,6-bis(4'-methylphenylsulfonyloxy)phthalonitrile (4.7 g, 10 mmol) was slowly added to the mixture in portions and the mixture was allowed to stir at room temperature for 16 h. After reaction, the mixture was poured into brine, stirred for 10 min, and extracted with dichloromethane (3 × 150 mL). The combined organic layers were dried by Na_2SO_4, filtrated, and concentrated under reduced pressure. The crude product was purified by column chromatography on silica gel (eluent: dichloromethane/petroleum ether). After recrystallization in

dichloromethane/methanol, bright-yellow crystalline solid (2.5 g, 82%) was obtained as product. ^{1}H NMR (400 MHz, $CDCl_3$) δ/ppm 7.50 (s, 2H), 3.02 (t, J = 7.3 Hz, 4H), 1.66 (p, J = 7.3 Hz, 4H), 1.48 (h, J = 7.3 Hz, 4H), 0.94 (t, J = 7.3 Hz, 6H). **(Supplementary Fig. S2)**

1.3.3 Synthesis of SBuPc

3,6-bis(butylthio)phthalonitrile (0.50 g, 1.65 mmol, 3 equiv.), copper(II) chloride (0.074 g, 0.55 mmol, 1 equiv.), DBU (1 mL), 1-pentanol (2 mL) were added to an oven-dried 25 mL round-bottom flask. The mixture was heated to reflux for 12 h. After cooling, MeOH/H_2O (1/1, 20 mL) was added to the mixture. The precipitate was filtered, washed with MeOH (3 × 5 mL), and redissolved in dichloromethane. Further purification was carried out by column chromatography on silica gel (eluent: dichloromethane/MeOH) to obtain purple solid (0.32 g, 61%) as product. MS (MALDI-TOF): m/z calcd. 1279.357 $[M]^+$; found 1279.417. **(Supplementary Fig. S3)** Elemental analysis calcd. (%) for $C_{64}H_{80}CuN_8S_8$: C, 59.99; H, 6.29; N, 8.74. Found: C, 60.24; H, 6.156; N, 8.53.

1.4 Perovskite Solar Cell Fabrications

Planar n-i-p perovskite solar cells (PSCs) were fabricated using ITO, SnO_2, perovskite, Spiro-OMeTAD/Pcs and gold (Au) as cathode, electron transport layer (ETL), light absorber layer, hole transport layer (HTL) and anode, respectively, according to a modified reported procedure.

1.4.1 Fabrication of ETL

ITO glasses (Yingkou OPV Tech New Energy Co., Ltd, China) were washed with cleaning fluid, deionized water, ethanol, acetone, and isopropanol sequentially. And then the ITO were treated with UV–ozone for 20 minutes. $SnCl_2{\cdot}2H_2O$ solution (0.1 M) was prepared by dissolving $SnCl_2{\cdot}2H_2O$ in anhydrous alcohol in a flask, then the solution was stirred at room temperature or 80 °C with the neck of flask sealed to prevent O_2 and H_2O into the solution for 3 hours. To obtained SnO_2 sol-gel solution, the just dissolved $SnCl_2{\cdot}2H_2O$ solution was transferred to an open reflux apparatus, then refluxing for overnight. When the reaction is over, the product was aged for over 24 hours at room temperature. The as-prepared sol-gel solution was then spin-coated (3000 rpm for 30 s) and thermal treatment at 150 °C for 30 minutes to form ETL and then the as-deposited ETL was treated with UV–ozone for 20 minutes. The 1 mg/mL NH_4Cl aqueous solution was spin-coated on the ETL surface, followed by thermal treatment at 80 °C for 20 minutes, then the as-deposited NH_4Cl was treated with UV–ozone for 20 minutes. Finally, the ITO/SnO_2 substrates were transferred to the Ar glove box (H_2O and O_2 content < 1 ppm) for perovskite layer deposition.

1.4.2 Fabrication of Perovskite Layer

The perovskite film was deposited on ITO/SnO_2 via a solvent engineering method. The perovskite precursor solution for $MAPbI_3$, the perovskite precursor solution comprised 1.43 mM $MAPbI_3$ (MAI: 227 mg; PbI_2: 659 mg), 1 mg KPF_6 and 5% mM MACl (5 mg) in 1 mL of DMF/DMSO (9:1, *v*/*v*). The $MAPbI_3$ film was prepared and spin-coated in two steps, namely, 1000 rpm for 5 s and 4000 rpm for 20 s, the acceleration is the maximum. Then, with 15 s of spin time remaining, anti-solvent (300 μL chlorobenzene for ITO area of 20 mm × 22 mm) was slowly dispensed onto the middle of the substrate and the films were annealed at 100 °C 15 minutes. The thickness of the as-fabricated $MAPbI_3$ layer was determined to be ~500 nm by Ambios Technology (Santa Cruz, CA) XP-2 profilometer. For $FAPbI_3$, the perovskite precursor solution comprised 1.6 mM $FAPbI_3$ (FAI: 275 mg; PbI_2: with 5% mole excessive lead iodide, 774 mg) and 20% mM MACl (22 mg) in 1 mL of DMF/DMSO (4:1, *v*/*v*). The $FAPbI_3$ film was prepared and spin-coated in two steps, namely, 1000 rpm for 5 s and 5000 rpm for 35 s, the acceleration is the maximum. Then, with 8–9 s of spin time remaining, anti-solvent (600 μL for ITO area of 20 mm × 22 mm) was slowly dispensed onto the middle of the substrate and the films were annealed at 150 °C 20 minutes. The anti-solvent is composed of ether and chlorobenzene in a ratio of 95:5. The thickness of the as-fabricated $FAPbI_3$ layer was determined to be ~800 nm by Ambios Technology (Santa Cruz, CA) XP-2 profilometer and cross-sectional SEM images. For $Cs_{0.04}Rb_{0.02}MA_{0.02}FA_{0.92}PbI_3$ (CsRbMAFA), the perovskite precursor solution comprised 1.8 mM CsRbMAFA (CsI: 18.71 mg; RbI: 7.65 mg; MAI: 5.72 mg; FAI: 248.78 mg; PbI_2: with 5% mole excessive lead iodide, 871.31 mg) and 14% mM MACl (17.02 mg) in 1 mL of DMF/DMSO (4:1, *v*/*v*). The CsRbMAFA film was prepared and spin-coated in two steps, namely, 1000 rpm for 5 s and 6000 rpm for 30 s, the acceleration is the maximum. Then, with 8–9 s of spin time remaining, anti-solvent (600 μL for ITO area of 20 mm × 22 mm) was slowly dispensed onto the middle of the substrate and the films were annealed at 110 °C 35 minutes. The anti-solvent is composed of ether and chlorobenzene in a ratio of 95:5. For $FAPbI_3$ and CsRbMAFA interfacial passivation of perovskite, the solution is dynamically spun on the perovskite film at 5000 rpm and annealed at 100 °C for 1 minute, the passivation solution is to dissolve 4 mg of PEAI and 1 mg of DDAI in 1 mL of isopropyl alcohol. And interface passivation is not applied to $MAPbI_3$. Finally, 0.5 mg/mL PMMA solution (in chlorobenzene) was dynamically spun onto 5000 rpm perovskite film and annealed at 100 °C for

5 minutes.

1.4.3 Fabrication of HTL

The HTL of doped Spiro-OMeTAD was deposited on the top of perovskite layer using spin-coating process (3000 rpm for 30 seconds) with a solution by dissolving 72.3 mg of Spiro-OMeTAD, 28.8 μL 4-tert-butylpyridine, 17.5 μL lithium bis(trifluoromethylsulfonyl)imide acetonitrile solution (520 mg mL^{-1}) into 1 mL chlorobenzene. The HTL of pristine Pc and Me_2Pc was prepared by thermal evaporation, a ~50 nm Pcs films was thermally evaporated under high vacuum (<10^{-5} Pa) on top of the devices and the thickness was monitored in-situ using quartz crystal. The HTL of SBuPc and SMePc was prepared by spin-coating using a solution (optimized concentration of 20 mg/mL in dichlorobenzene) with a speed of 2500 rpm for 60 seconds to obtain a Pcs film of thickness ~60 nm determined from ellipsometry. After the HTL deposition, the 8 nm MoO_3 and 100 nm Au electrode was thermally evaporated under high vacuum (<10^{-5} Pa) on top of the devices. The device size areas were 0.10 cm^2. When measuring, a 3.97 mm^2 non-reflective mask was used to define the accurate active cell area. For thermal annealing, the obtained PSCs based on Pcs based HTL were heated under optimized condition of 85 °C for 22 hours in Ar atmosphere.

1.5 Film characterization

Thin film grazing incidence X-ray diffraction (GIXRD) measurements of the perovskite were performed on a Smartlab 9-kW diffractometer with a Göbel mirror attachment. Irradiation of the parallel CuKα1,2 X-ray beams was fixed at a grazing incident angle (θ) of 0.500°. The detector was independently moved to collect diffraction data in the 2θ range (4°–11° and 20°–28°) with a step size of 0.03° (2θ) at a fixed speed of 0.5 sec/step.

The steady-state photoluminescence spectra and TRPL decay curve measurements for perovskite films (Glass/perovskite/HTL) were performed on an FLS1000 spectrometer (Edinburgh Instruments) with excitation from a 475-nm pulsed laser. The samples were excited from the perovskite side under ambient conditions. The TRPL data were fitted with a biexponential function as following:

$$f(t) = A_1 exp\left(\frac{-t}{\tau_1}\right) + A_2 exp\left(\frac{-t}{\tau_2}\right)$$

where τ_1 and τ_2 represent fast-decay and slow-decay components, respectively.

Ultraviolet photo-electron spectroscopy (UPS) and X-ray photoelectron spectroscopy (XPS)

measurements were performed using an ultrahigh vacuum surface analysis system equipped with an ULVAC-PHI 5000 VersaProbe III spectrometer. UPS was performed with He I (21.22 eV) as the excitation source at an energy resolution of 50 meV. XPS used monochromatic Al Kα radiation (1,486.6 eV). All experiments were calibrated to the Fermi edge of an atomically clean gold surface.

1.6 TA and TR spectroscopy measurement

The fundamental beam (800 nm, Coherent Astrella) is split in two beams. One beam is sent to an optical parametric amplifier (TOPAS, Light conversion) to generate the pump pulse, and its intensity is attenuated by two neutral density filter wheels. The other 800 nm beam is focused into a sapphire crystal to generate white light probe (450-810 nm) and detected with a CMOS detector (Timetech, TA-100). The probe pulses are delayed in time with respect to the pump pulses using a motorized translation stage mounted with a retroreflecting mirror. Probe delay can be up to ~5 ns, tuned by a delay line. The probe size is ~180 × 125 μm, and pump beam size is ~340 × 440 μm for 480 nm, ~730 × 670 μm for 600 nm and ~520 × 490 μm for 750 nm. The beam size is defined as the radius of an aperture that contains ($1/e^2$) of the total power. The pump and probe are spatially overlapped on the surface of the sample. For TR measurement, the incident angle for pump is around 0° and probe is around 45°.

1.7 TR kinetics diffusion-surface extraction modelling

For any sample, the kinetics of different pump light excitation conditions are different, because the perovskite sample has different absorption coefficients for different wavelengths of light, which leads to different initial carrier distributions in the sample when the sample is first excited. This method is modified from literature.[4,5]

According to the Beer–Lambert law, a pump with higher photon energy always leads to a larger gradient of the initial photocarrier density and thus a faster surface decay dynamics due to a larger diffusion rate. To quantitatively describe the carrier density evolvement under the various optical excitation conditions, a one-dimensional diffusion equation is employed,

$$\frac{\partial N(x,t)}{\partial t} = D \times \frac{\partial^2 N(x,t)}{\partial x^2} - \frac{N(x,t)}{\tau_B} \#(1)$$

where N(x, t) is the carrier density as a function of depth (x) and time (t), D is the ambipolar diffusion coefficient and τ_B is the bulk carrier lifetime. In comparison with the timescale for carrier diffusion, the pulsed carrier generation is assumed to be instantaneous, and the initial condition for

equation (1) is then given by

$$N(x,0) = N_0\, e^{-\alpha x} \#(2)$$

where N_0 is the initial surface carrier density, such that $N_0 = \alpha\,(1 - R)J_0$, where J_0 is the pump fluence and R is the reflectance at the pump-photon energy. If the traces are normalized, then N_0 is equal to 1. The values for the absorption coefficient α at different pump-photon energies for both samples are known.

For the polycrystalline samples, the boundary conditions are described as

$$\frac{\partial N(x,t)}{\partial x}\Big|_{x=0} = \frac{S_F}{D} \times N(0,t) \#(3)$$

and

$$\frac{\partial N(x,t)}{\partial x}\Big|_{x=L} = -\frac{S_L}{D} \times N(L,t) \#(4)$$

where L is the thickness of the perovskite layer that is orders of magnitude thicker than the optical penetration depth plus carrier diffusion length, and S is the surface recombiniation velocity (SRV). In addition, when the HTL is added, surface hole extraction occurs, which decreases the carrier concentration in the perovskite film, and this can be considered to be the effective surface extraction velocity (SEV). For higher carrier density experiments, the diffusion constant is held at constant where SEV is allowed to vary. The electron mobility in perovskites could be 10 times larger than the holes, therefore, the ambipolar diffusion will be limited by holes.

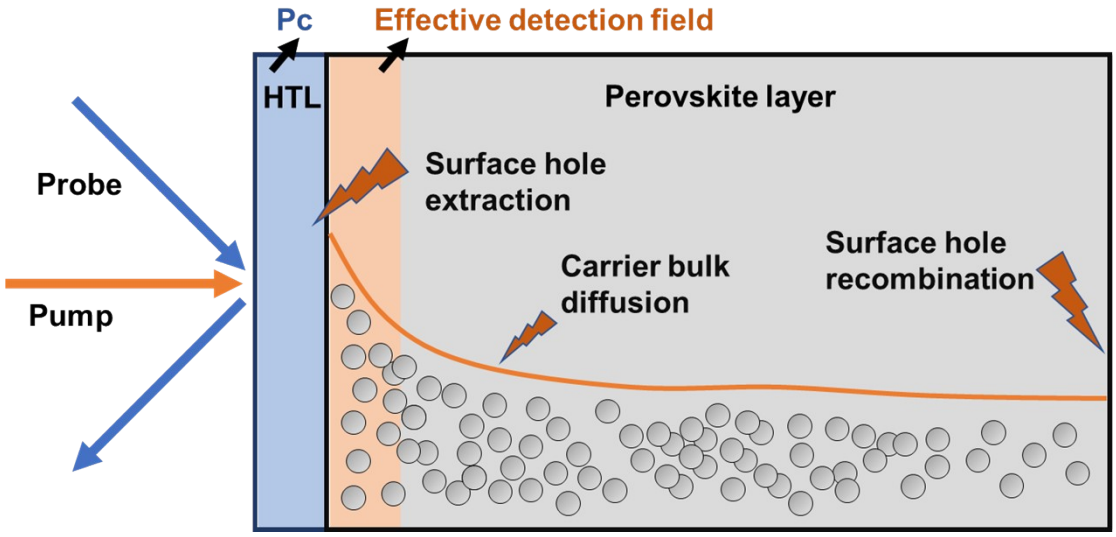

Scheme S2. Schematic of diffusion-recombination/extraction model

1.8 Device characterization

A Keithley 2400 source measure unit was used and an Oriel xenon lamp (450 W) with an AM 1.5 filter, to characterize solar cells in air under AM 1.5G illumination of 100 mW cm^{-2} (Oriel 1 kW Newport solar simulator), calibrated with a KG5 filter certified by the National Renewable Energy Laboratory. Current density–voltage (J–V) curves of all devices (active area, 3.97 mm^2) were measured at a scan rate of 0.1 V s^{-1}.

Operational stability tests were performed at the MPP for the unencapsulated devices under AM 1.5G illumination (100 mW/cm^2) at 60±10 °C in a N_2 atmosphere within a light-emitting diode (LED)-based solar simulator. The bias at the MPP was calculated and then applied automatically. The light intensity was calibrated versus a standard silicon reference cell supplied by Newport.

The concentrated light source was obtained by focusing a xenon lamp (Solar Simulator, 94063A model) simulated white-light source including an AM 1.5G filter. The light intensity was modulated by a set of Fresnel lenses with different focal lengths and a height shift stage that can be adjusted, and the exact numeric value was determined using a solar power meter (PL-MW2000, Beijing Perfectlight Technology Co., Ltd). During the test, the cell temperature is controlled at room temperature by blowing the surface of the PSCs device with a high-speed air gas flow. To avoid the effect of parasitic resistance, the active area of the perovskite solar cells was reduced to ~1mm^2. The J–V curves were recorded with a 2601B system source meter (Keithley Instruments) via a four-wire connection mode, which overcomes resistive losses in the electrical cables, and contact resistance between the connecting pins.

1.9 Computational methods

The calculations were performed using the spin-polarized density functional theory (DFT) methods implemented in the CP2K package. The Perdew-Burke-Ernzerhof (PBE) functional, which is a generalized gradient approximation, was employed to describe the exchange and correlation interactions of valence electrons. The wave functions were expanded using a molecularly optimized double-zeta Gaussian basis set with a cutoff energy of 400 Ry. Dispersion interactions were accounted for using Grimme's D3 dispersion corrections. In each self-consistent field (SCF) iteration step, the energy was converged to 10^{-6} Ry, while the atomic forces were constrained to be less than 0.02 eV/Å.

The perovskite model had dimensions of 39.00 × 39.00 × 43.50 $Å^3$, and a vacuum of 15.0 Å inserted along the [001] direction to avoid unphysical interactions between the slab layers. The ab

initio molecular dynamics (AIMD) simulations were performed in the canonical (NVT) ensemble using Nose-Hoover thermostats with a time step of 1.0 fs at a typical temperature of 300 K. During the simulation, DFT-optimized structures were adopted as initial structures to achieve equilibration trajectories for approximately 7 ps. The radial distribution functions (RDFs) between the S atoms in the Pcs molecules and Pb atoms on perovskite surface was analyzed, and the date were collected from the final 5 ps. Charge density difference ($\Delta\rho$) of Pcs molecules on the perovskite were calculated as, $\Delta\rho=\rho_{(Pcs/PVK)}-\rho_{(Pcs)}-\rho_{(PVK)}$. The charge density accumulation and depletion areas are indicated in yellow and cyan, respectively. The isosurface value is set to ±0.004 e/Å^3.

2. Supplementary Figs. S1 to S31

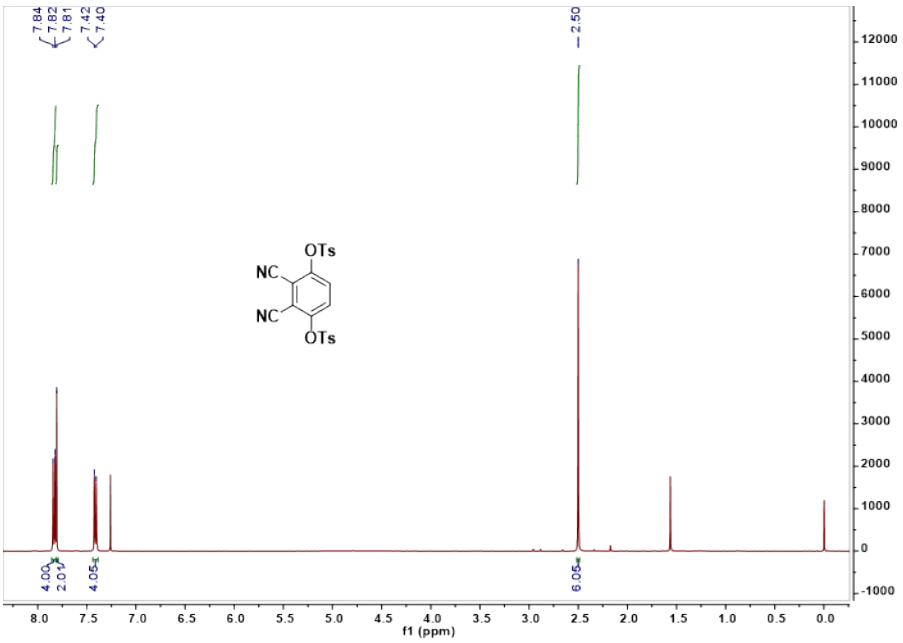

Figure S1. ^{1}H NMR spectrum (400 MHz, $CDCl_3$) of 3,6-bis(4'-methylphenylsulfonyloxy)phthalonitrile.

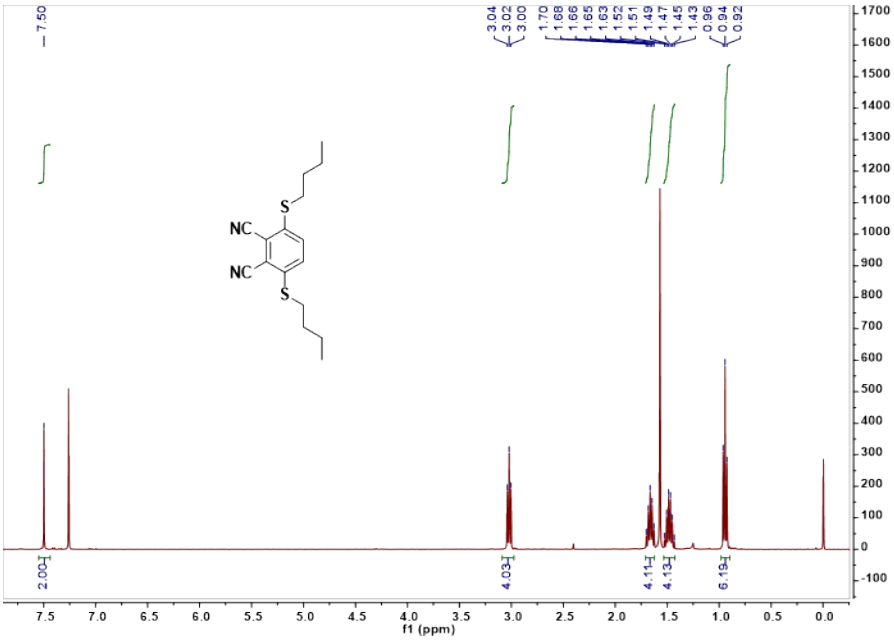

Figure S2. ^{1}H NMR spectrum (400 MHz, $CDCl_3$) of 3,6-bis(butylthio)phthalonitrile.

Cpd.	Experiment	Elemental Analysis		
		C%	H%	N%
CuPc-NPSC4	Calculated Value	59.99	6.29	8.74
	Experiment 1	60.24	6.156	8.53
	Experiment 2	60.42	6.229	8.59

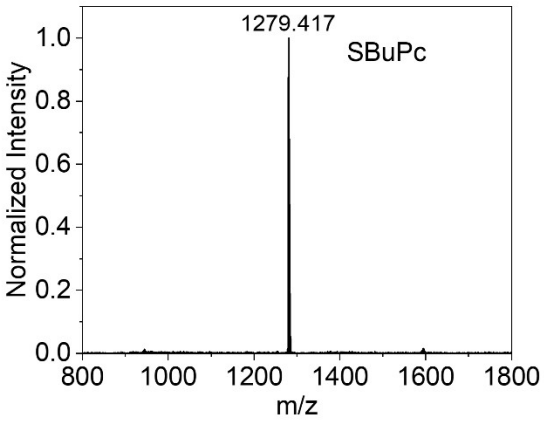

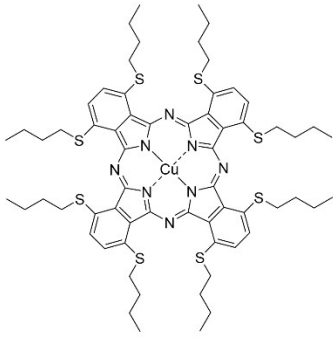

Exact mass: 1279.3568
MALDI-TOF: 1279.417

Figure S3. Elemental analysis and MALDI-TOF mass spectrum of SBuPc.

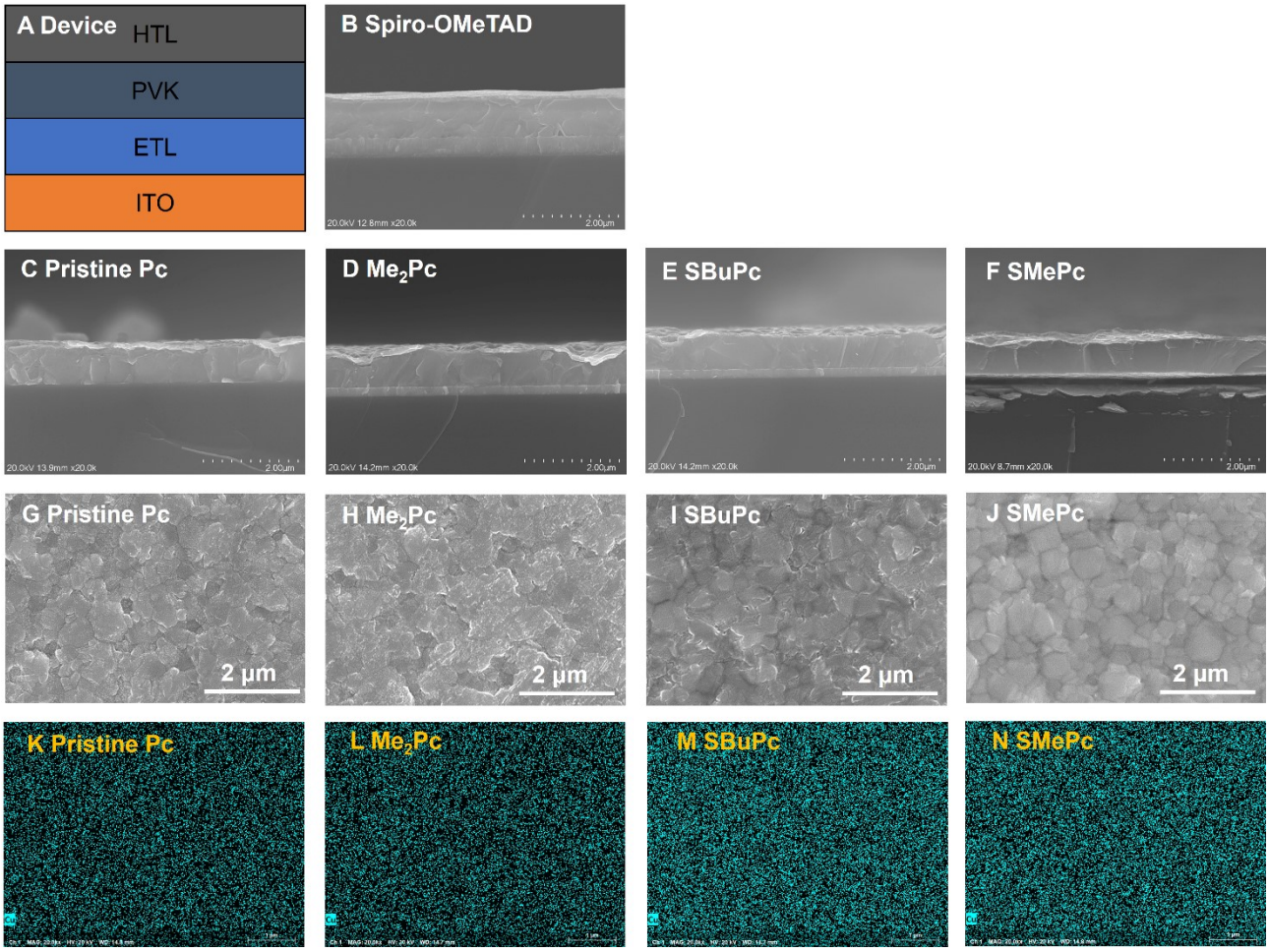

Figure S4. (**A**) Planar n-i-p PSC configuration. (**B** to **F**) Cross-sectional SEM images of the $FAPbI_3$ based perovskite solar cell devices. (**G** to **J**) Overhead view SEM images of phthalocyanines deposited on $FAPbI_3$. The grains are possibly perovskites. (**K** to **N**) EDS mapping data of the Cu element for four phthalocyanines deposited on $FAPbI_3$.

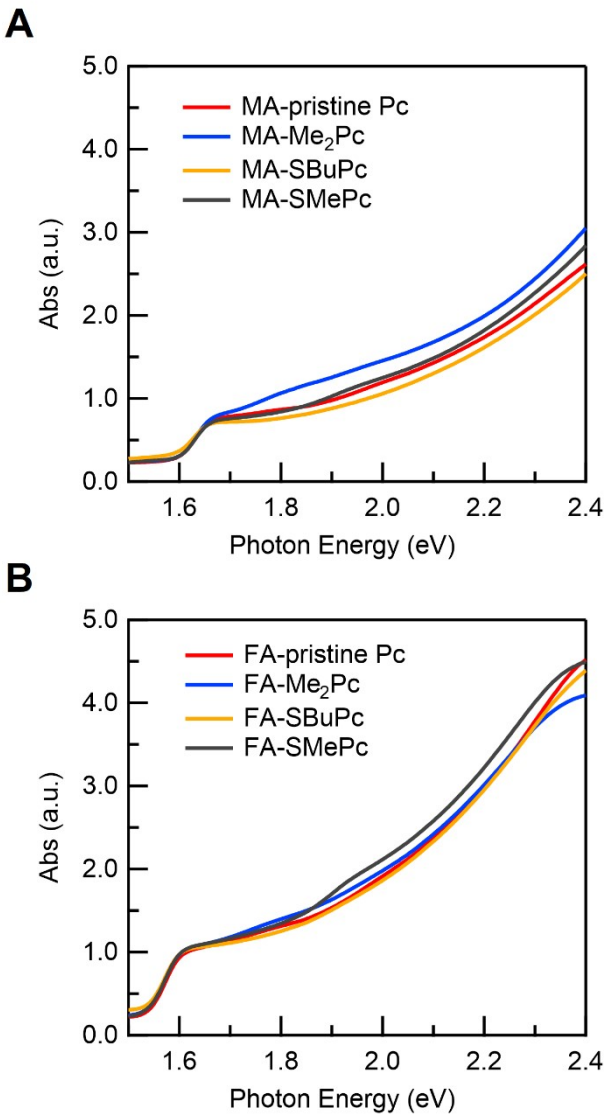

Figure S5. UV-vis spectra of MA and FA based perovskite films.

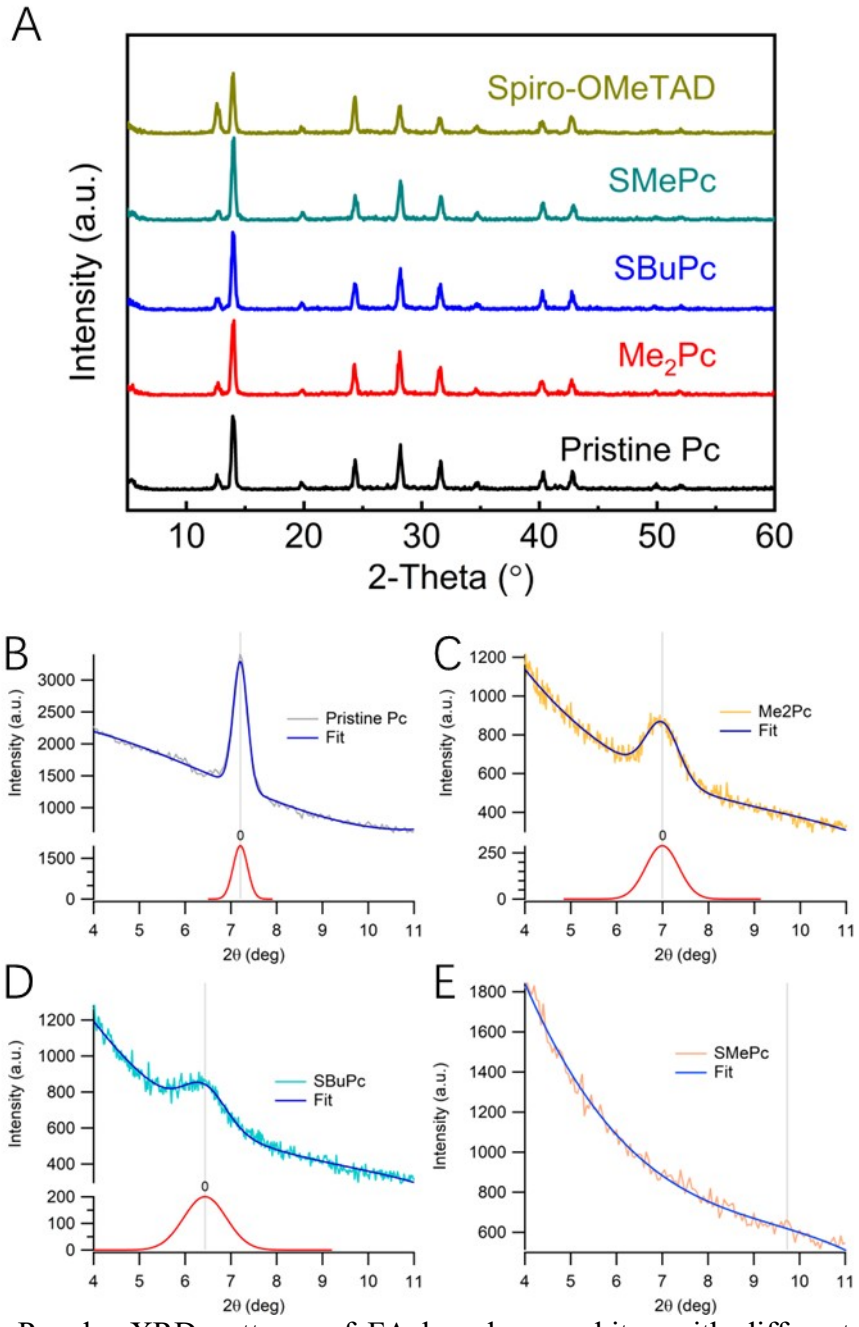

Figure S6. A. Powder XRD patterns of FA based perovskites with different phthalocyanine molecules. B-E GIXRD fittings at small angles for the different phthalocyanine molecules.

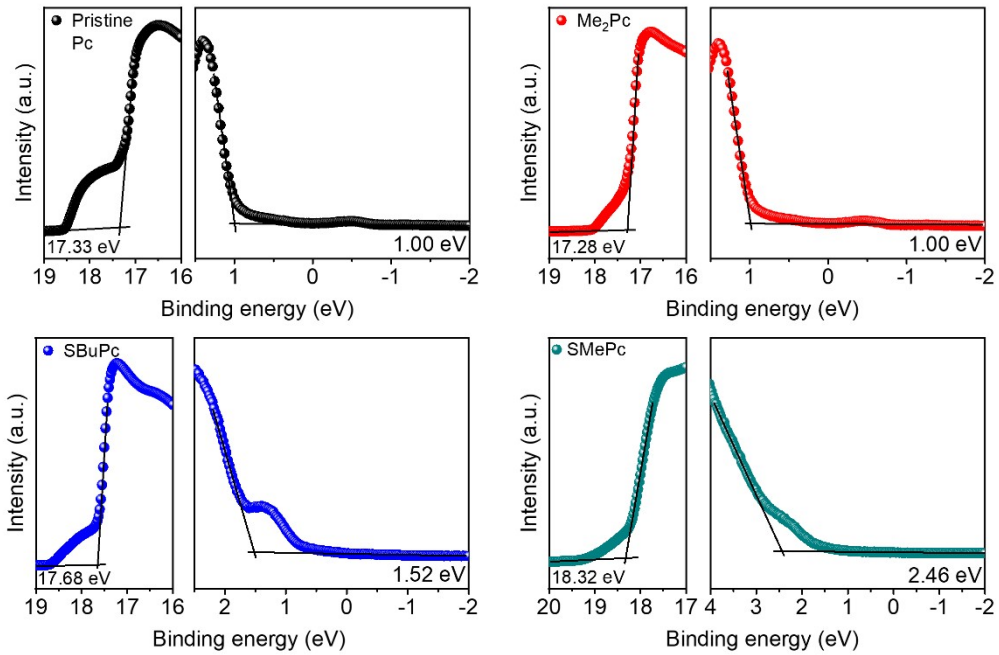

Figure S7. UPS of four phthalocyanine molecules.

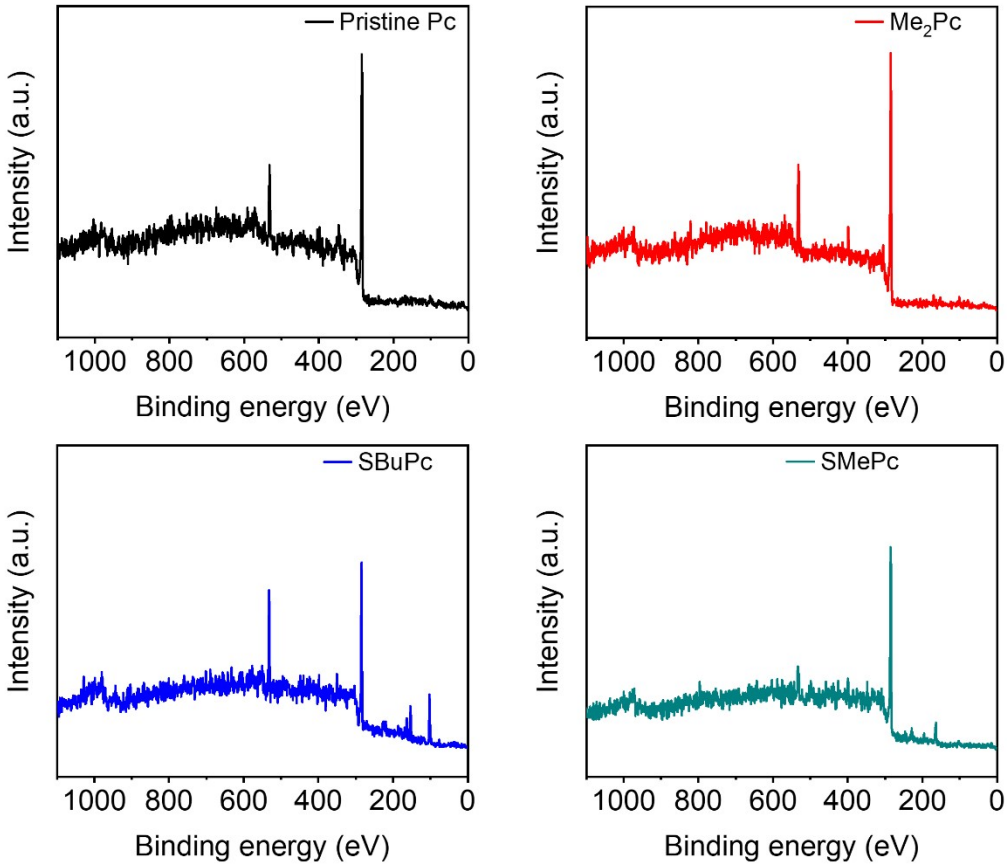

Figure S8. XPS data of powder phthalocyanine molecules.

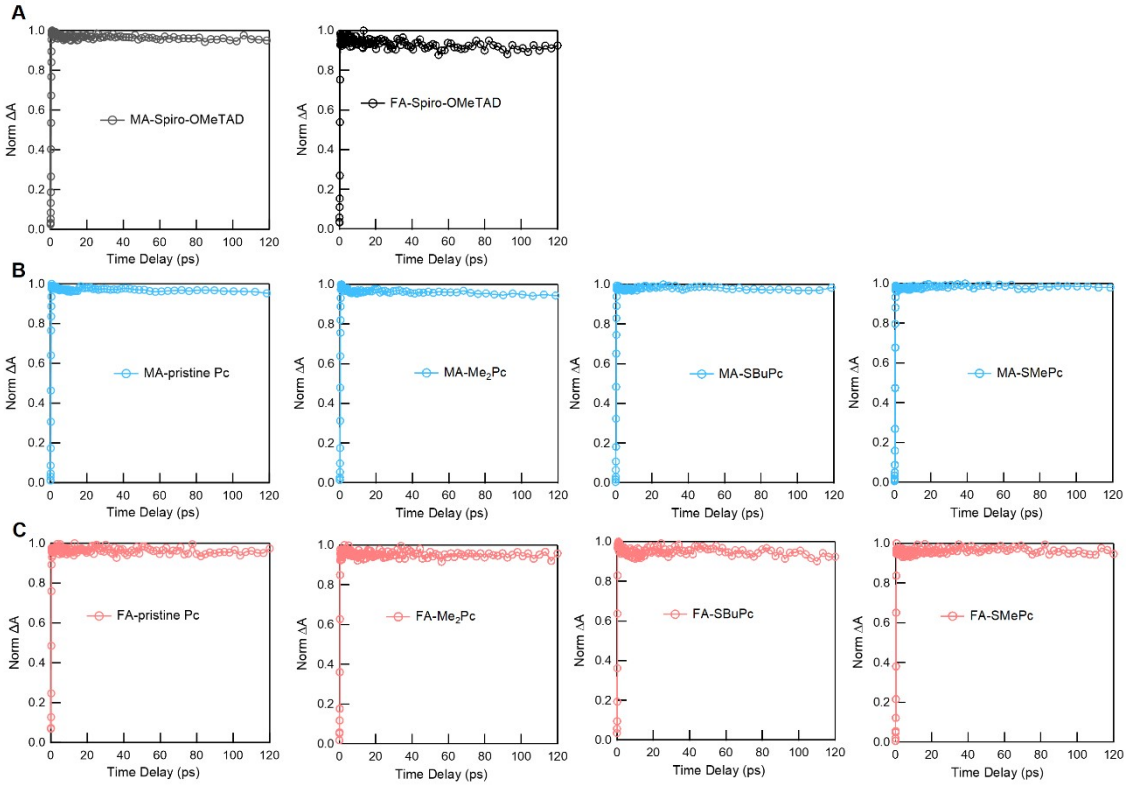

Figure S9. TA kinetics of perovskites excited with 1.65 eV at ~10^{17} cm^{-3} carrier concentration. (**A**) MA and FA based perovskite with Spiro-OMeTAD. (**B**) MA based perovskite with phthalocyanine molecules. (**C**) FA based perovskite with phthalocyanine molecules.

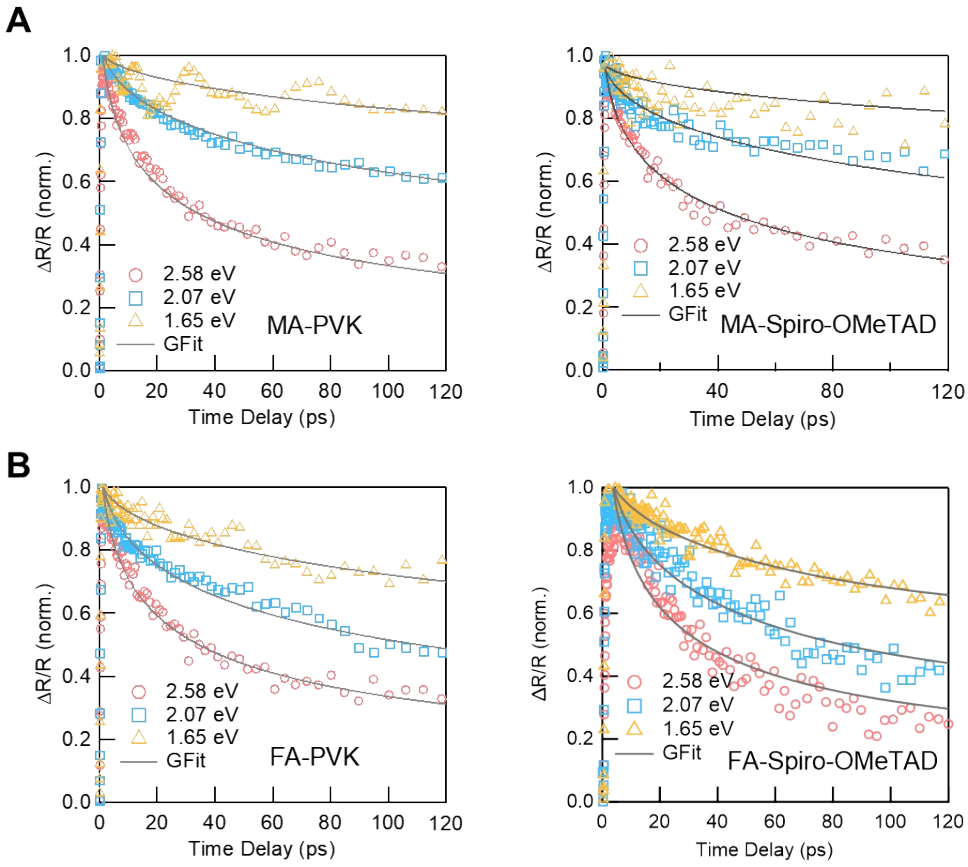

Figure S10. Transient reflection kinetics excited with 2.58 eV, 2.07 eV and 1.65 eV pump at ~10^{17} cm^{-3} carrier density for MA (**A**) and FA (**B**) based perovskites with pure perovskite, Spiro-OMeTAD.

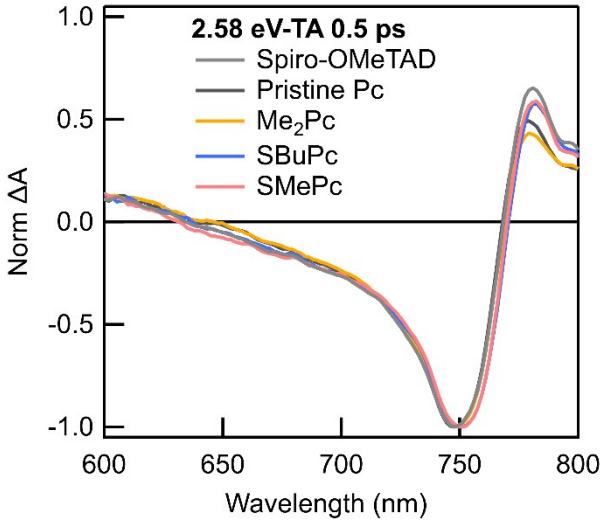

Figure S11. TA spectra excited with 2.58 eV with 1.2×10^{19} cm^{-3} carrier density for perovskites with HTLs.

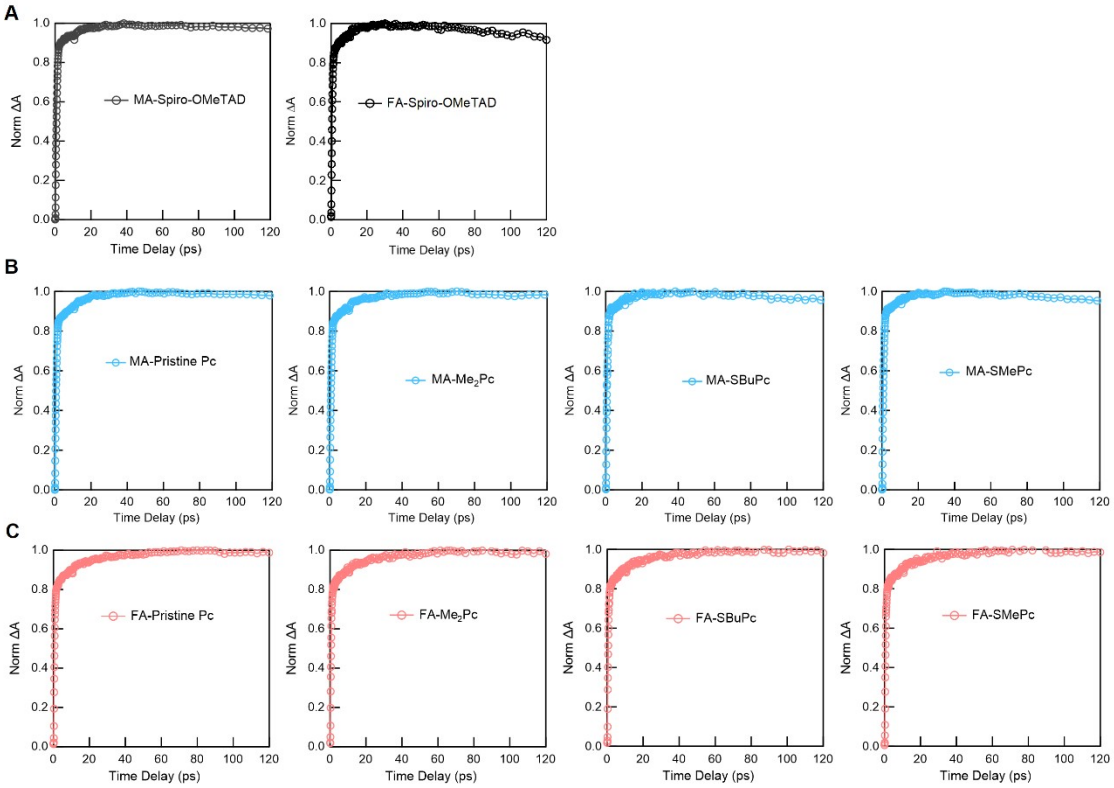

Figure S12. TA kinetics of perovskites excited with 2.58 eV at ~10^{19} cm^{-3} carrier concentration. (**A**) MA and FA based perovskite with Spiro-OMeTAD. (**B**) MA based perovskite with phthalocyanine molecules. (**C**) FA based perovskite with phthalocyanine molecules.

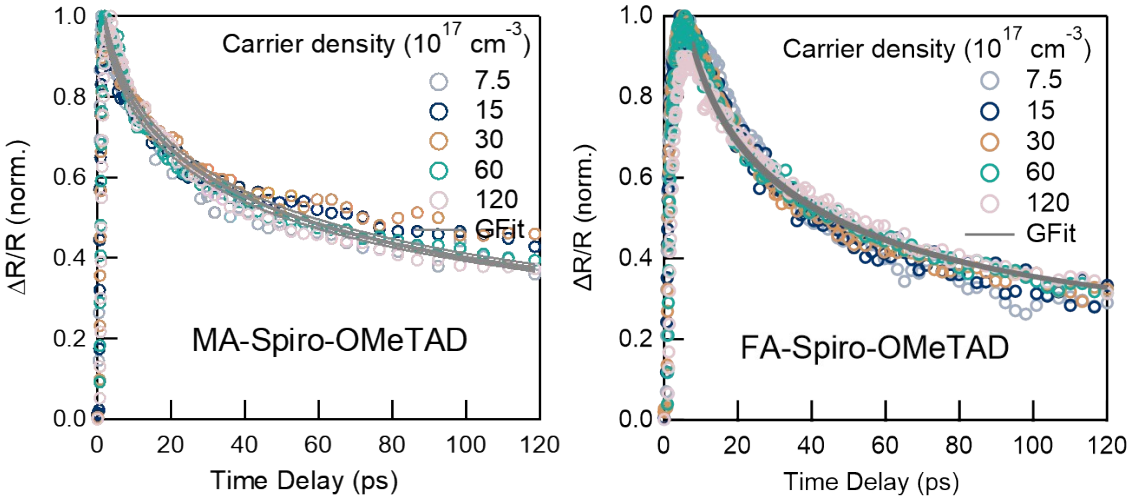

Figure S13. TR kinetics under various carrier densities excited at 2.58 eV pump energy, modelled with SEV for perovskites with Spiro-OMeTAD.

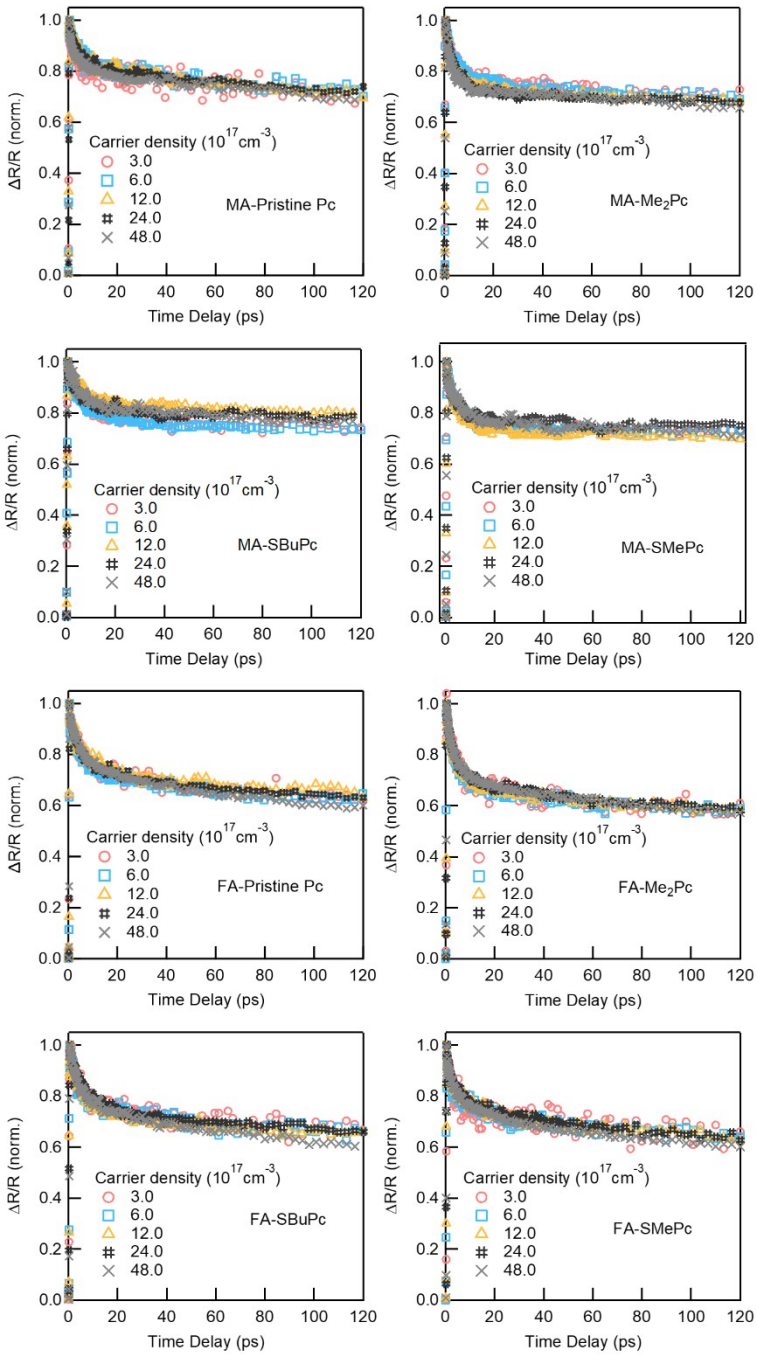

Figure S14. 1.65 eV pump power dependence TR kinetics result of MA and FA based perovskites**.** No change in carrier extraction velocity is observed.

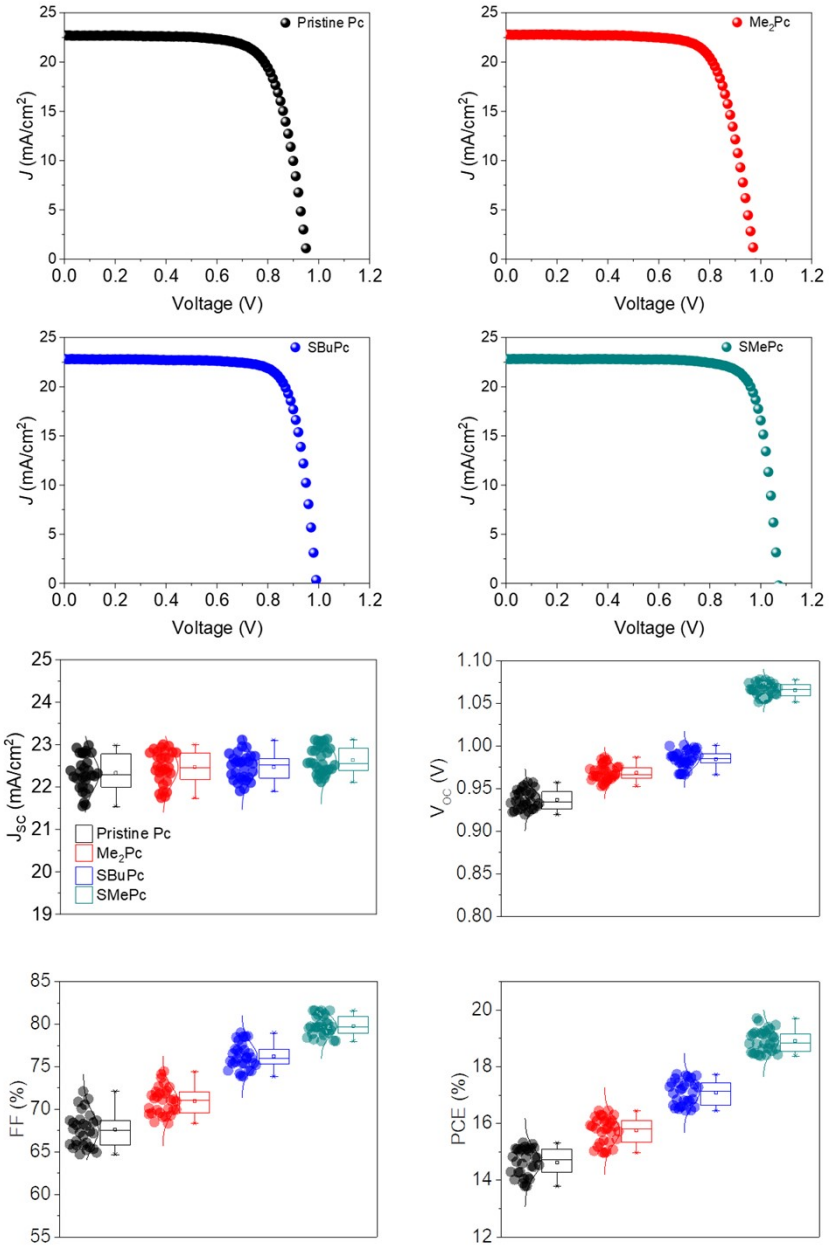

Figure S15. J-V curves and box plots of MA based PSCs.

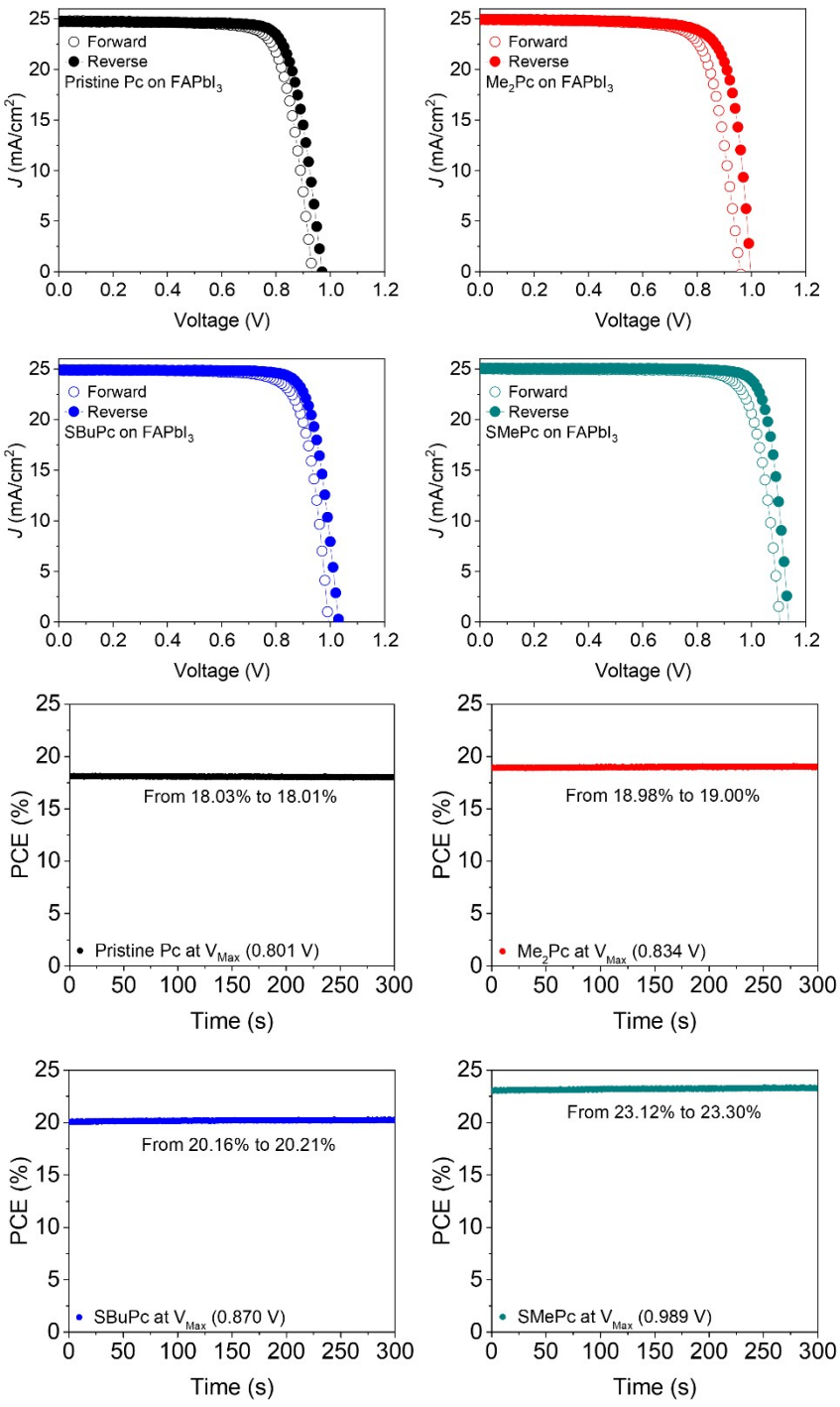

Figure S16. J-V curves and stabilized power output (SPO) data of FAPbI3 based PSCs.

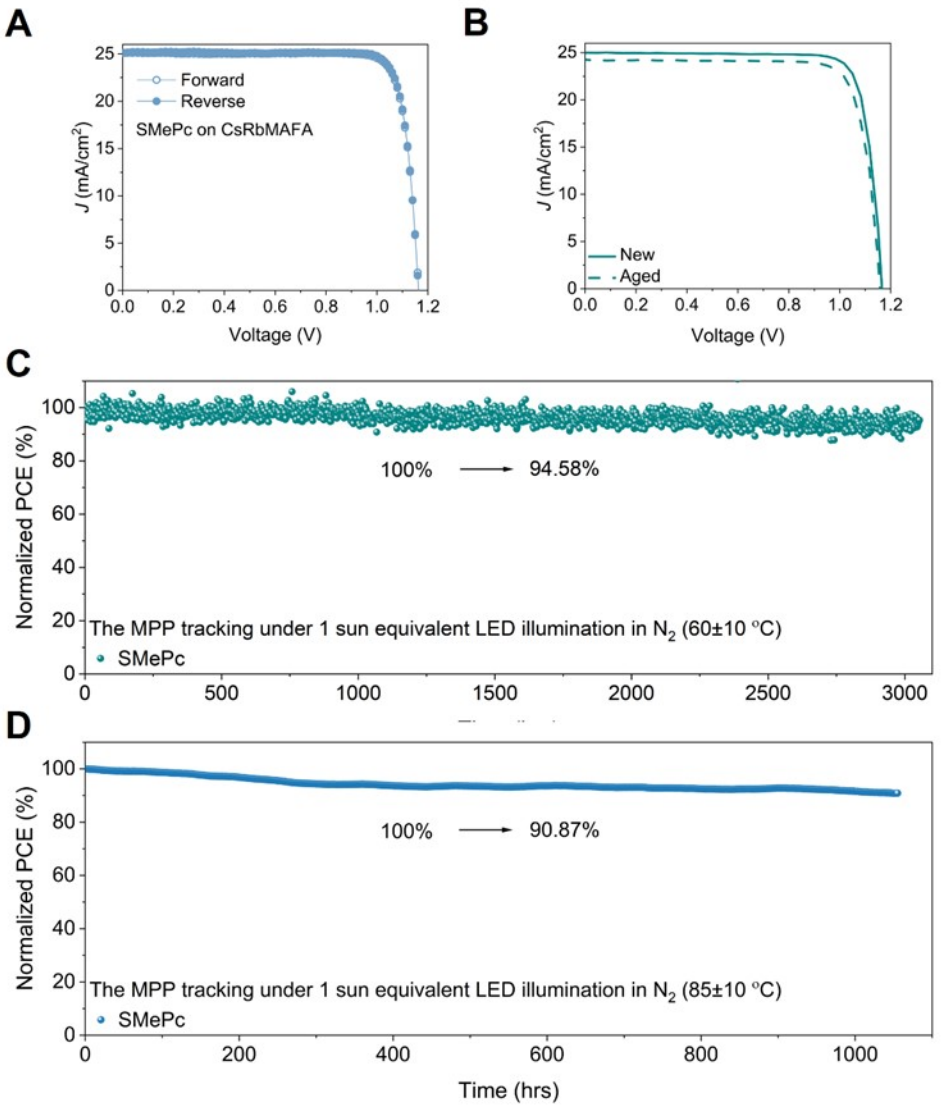

Sample	*Jsc* (mA/cm²)	*Voc* (V)	FF (%)	PCE (%)
New	24.98	1.166	83.33	24.27
Aged	24.22	1.158	81.81	22.95

Figure S17. (A) J-V curves of the champion device with SMePc as HTL on FA rich CsRbMAFA perovskite film. **(B)** Initial and aged performance of the PSCs for stability measurement at 60℃. Stability of perovskite devices with MPP tracking at 1 sun intensity at **(C)** 60℃ **(D)** 85℃.

230017163974

中国认可
国际互认
检测
TESTING
CNAS L8490

Test and Calibration Center of New Energy Device and Module,
Shanghai Institute of Microsystem and Information Technology,
Chinese Academy of Sciences (SIMIT)

Measurement Report

Report No. 23TR071307

Client Name	Southern University of Science and Technology (SUSTech)
Client Address	No. 1088 Xueyuan Avenue, Nanshan District, Shenzhen, China
Sample	Perovskite solar cell
Manufacturer	Zongxiang Xu's Group, SUSTech
Measurement Date	13th July, 2023

Performed by:	Qiang Shi Qiang Shi	**Date:** 13/07/2023
Reviewed by:	Wenjie Zhao Wenjie Zhao	**Date:** 13/07/2023
Approved by:	Yucheng Liu Yucheng Liu	**Date:** 13/07/2023

Address: No.235 Chengbei Road, Jiading, Shanghai **Post Code:**201800

E-mail: solarcell@mail.sim.ac.cn **Tel:** +86-021-69976921

Sample Information

Sample Type	Perovskite Solar Cell
Serial No.	9-A#
Lab Internal No.	23071301-7#
Measurement Item	I-V characteristic
Measurement Environment	25.3±2.0°C, 44.1±5.0%R.H

Measurement of I-V characteristic

Reference cell	PVM 1121
Reference cell Type	mono-Si, WPVS, calibrated by NREL (Certificate No. ISO 2075)
Calibration Value/Date of Calibration for Reference cell	144.53mA/ Feb. 2023
Measurement Conditions	Standard Test Condition (STC): Spectral Distribution: AM1.5 according to IEC 60904-3 Ed.3, Irradiance: 1000±50W/m^2, Temperature: 25±2°C
Measurement Equipment/ Date of Calibration	AAA Steady State Solar Simulator (YSS-T155-2M) / July.2022 IV test system (ADCMT 6246) / June. 2023 SR Measurement system (CEP-25ML-CAS) / April.2023 Measuring Microscope (MF-B2017C) / July.2022
Measurement Method	I-V Measurement: Logarithmic sweep in both directions (Voc to Isc and Isc to Voc) during one flash based on IEC 60904-1:2020; Spectral Mismatch factor was calculated according to IEC 60904-7 and I-V correction according to IEC 60891.
Measurement Uncertainty	Area: 1.0%(k=2); Isc: 1.8%(k=2); Voc: 1.0%(k=2); Pmax: 2.3%(k=2); Eff: 2.5%(k=2)

Report No. 23TR071307

====Measurement Results ====

	Forward Scan (Isc to Voc)	Reverse Scan (Voc to Isc)
Area	3.97 mm^2	
Isc	0.995 mA	0.996 mA
Voc	1.159 V	1.161 V
Pmax	0.969 mW	0.970 mW
Ipm	0.942 mA	0.946 mA
Vpm	1.029 V	1.025 V
FF	84.03 %	83.80 %
Eff	24.40 %	24.43 %

- Spectral Mismatch Factor: SMM=0.9867.
- Designated illumination area defined by a thin metal mask was measured by the measuring microscope.
- Test results listed in this measurement report refer exclusively to the mentioned measured sample.
- The results apply only at the time of the test, and do not imply future performance.

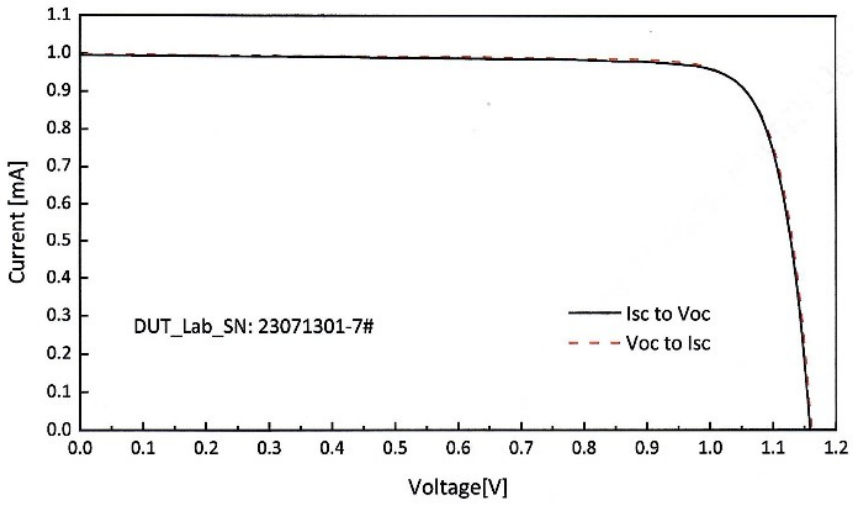

Fig.1 I-V curves of the measured sample

-------End of Report-------

3 / 3

Figure S18. Certification results for FA rich CsRbMAFA perovskite with SMePc as HTL.

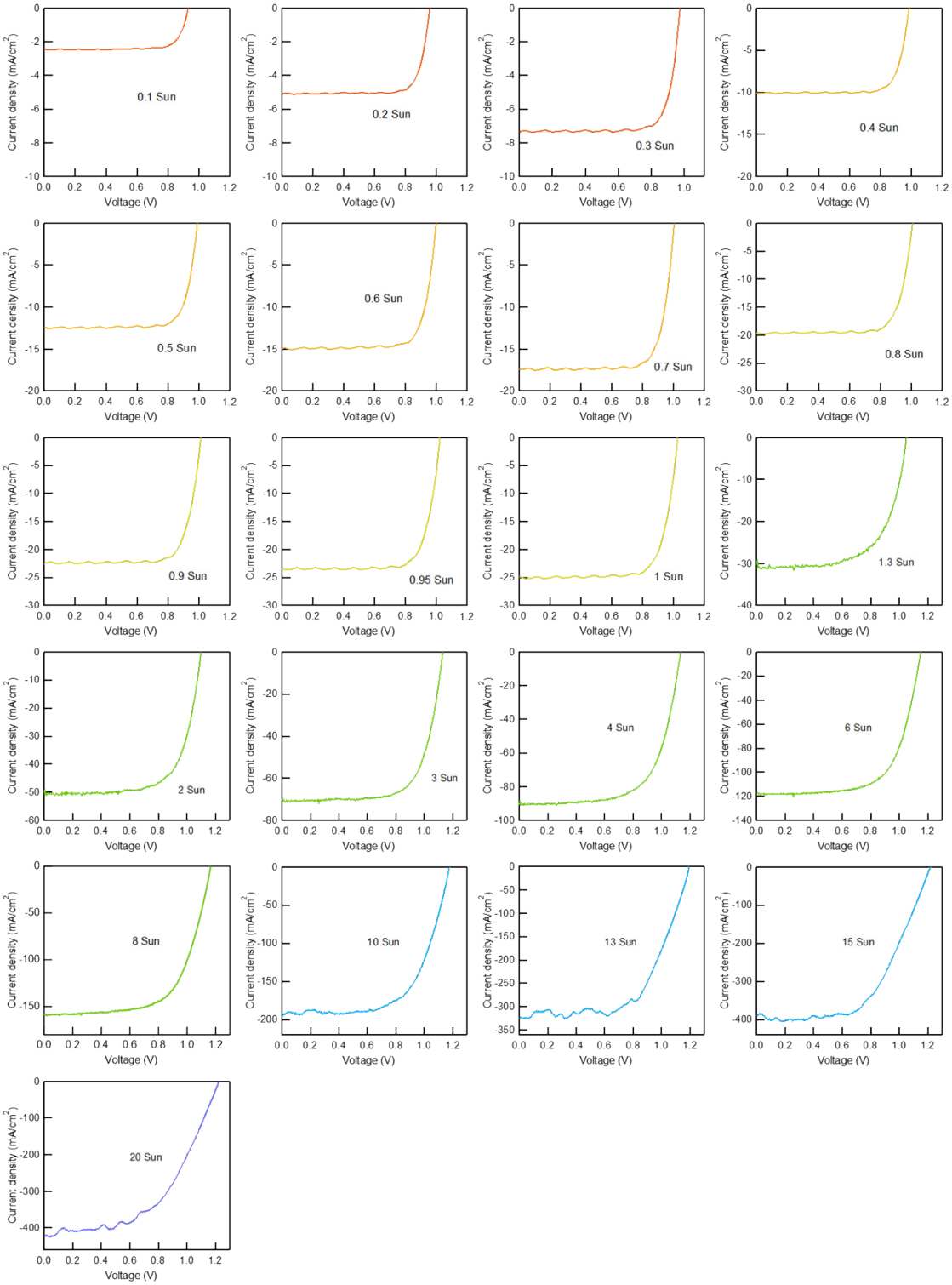

Figure S19. Measured J−V characteristics of the device with SBuPc under simulated concentrated AM 1.5 G sunlight at various irradiance levels for $FAPbI_3$.

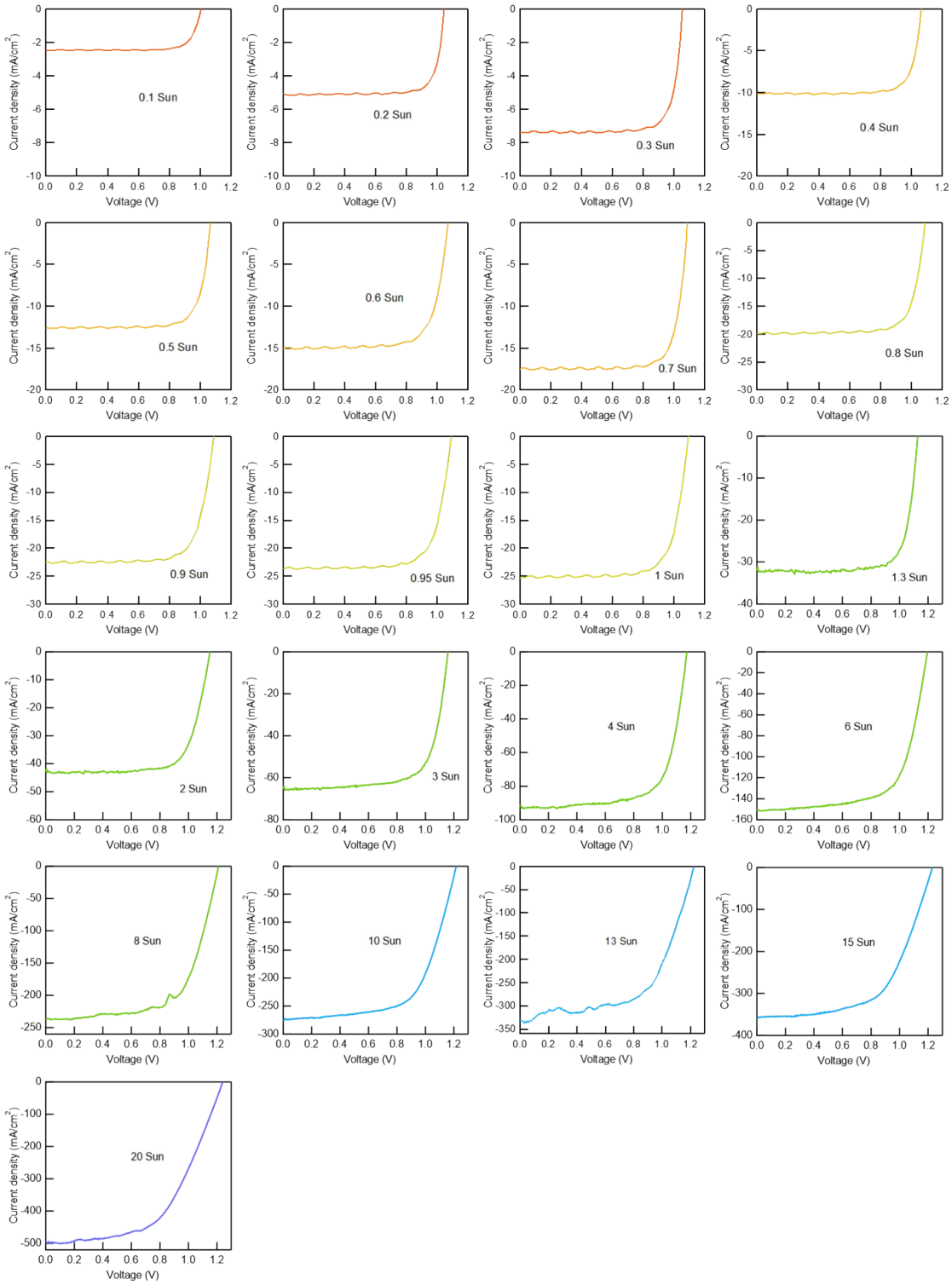

Figure S20. Measured J−V characteristics of the device with SMePc under simulated concentrated AM 1.5 G sunlight at various irradiance levels for $FAPbI_3$.

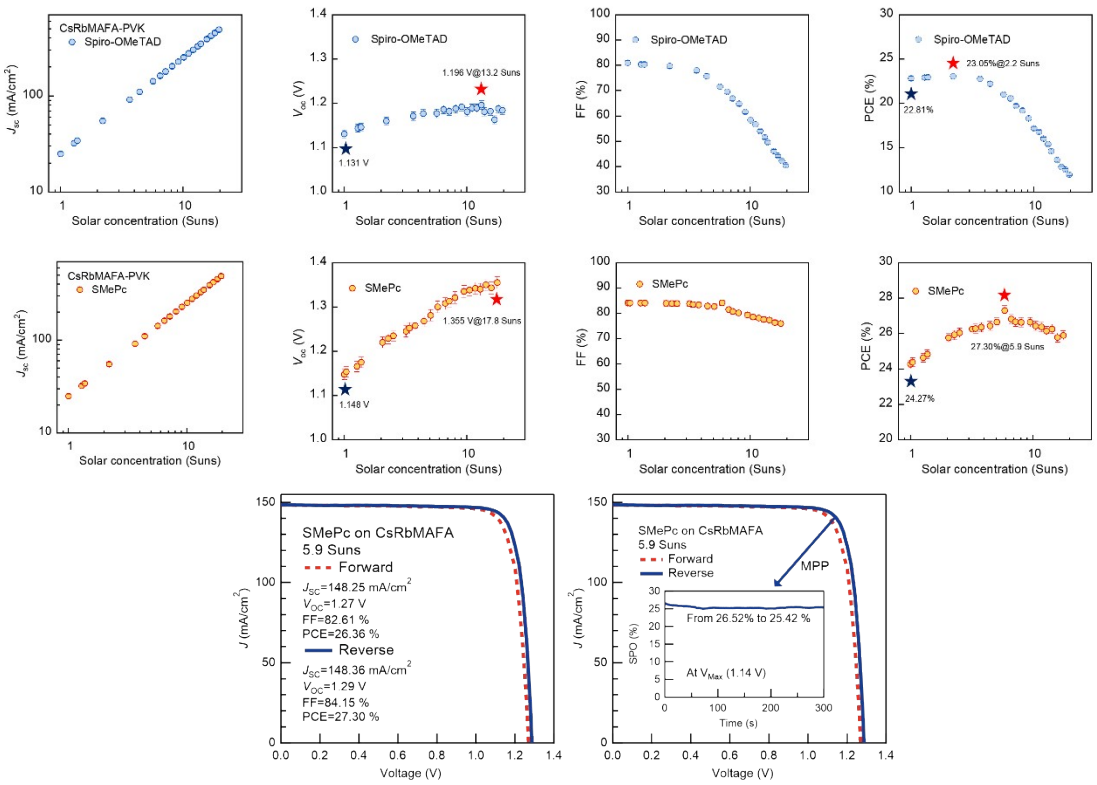

Figure S21. Concentrator PV device performance of champion FA rich perovskites with Spiro-OMeTAD and SMePc as HTL at various solar concentration.

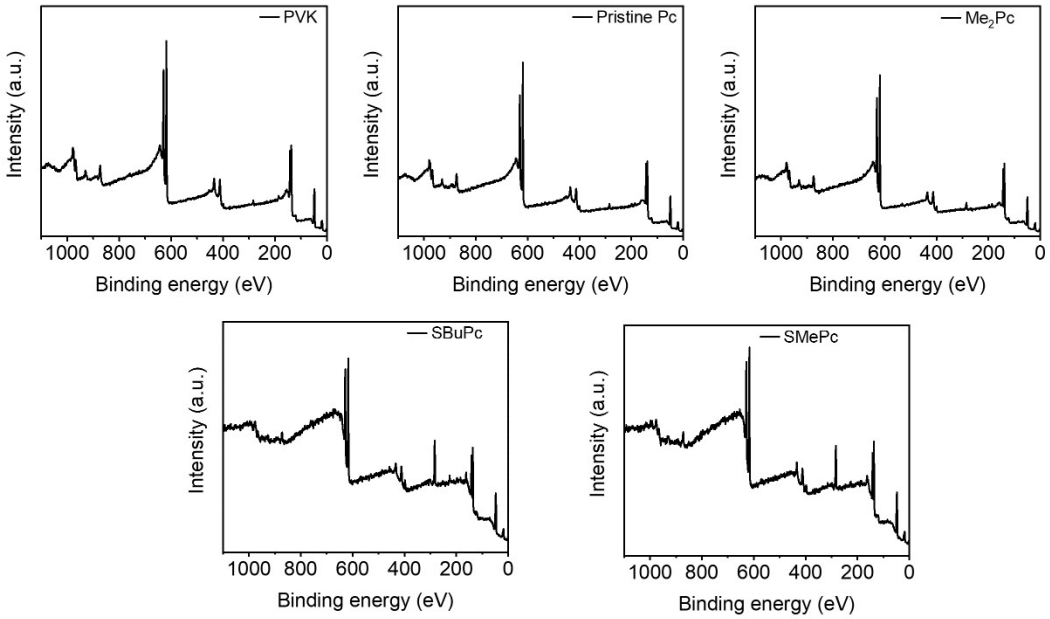

Figure S22. Full XPS scan survey spectra for FA based samples with and without Pcs.

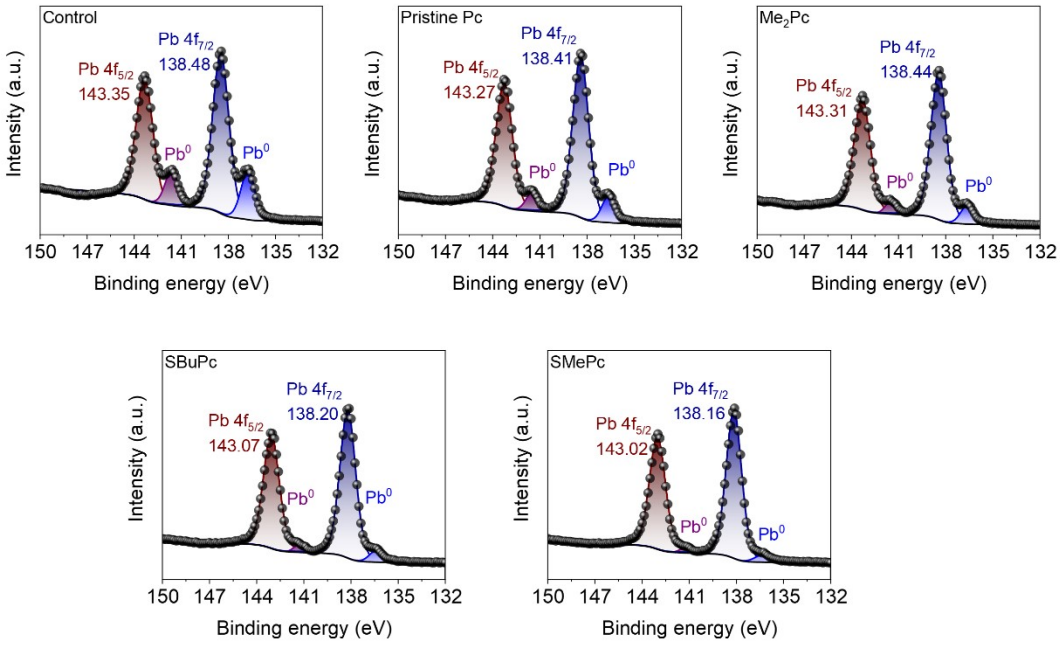

Figure S23. Pb 4f XPS spectra for perovskite samples without HTL (Control) and with HTLs (pristine Pc, Me_2Pc, SBuPc and SMePc).

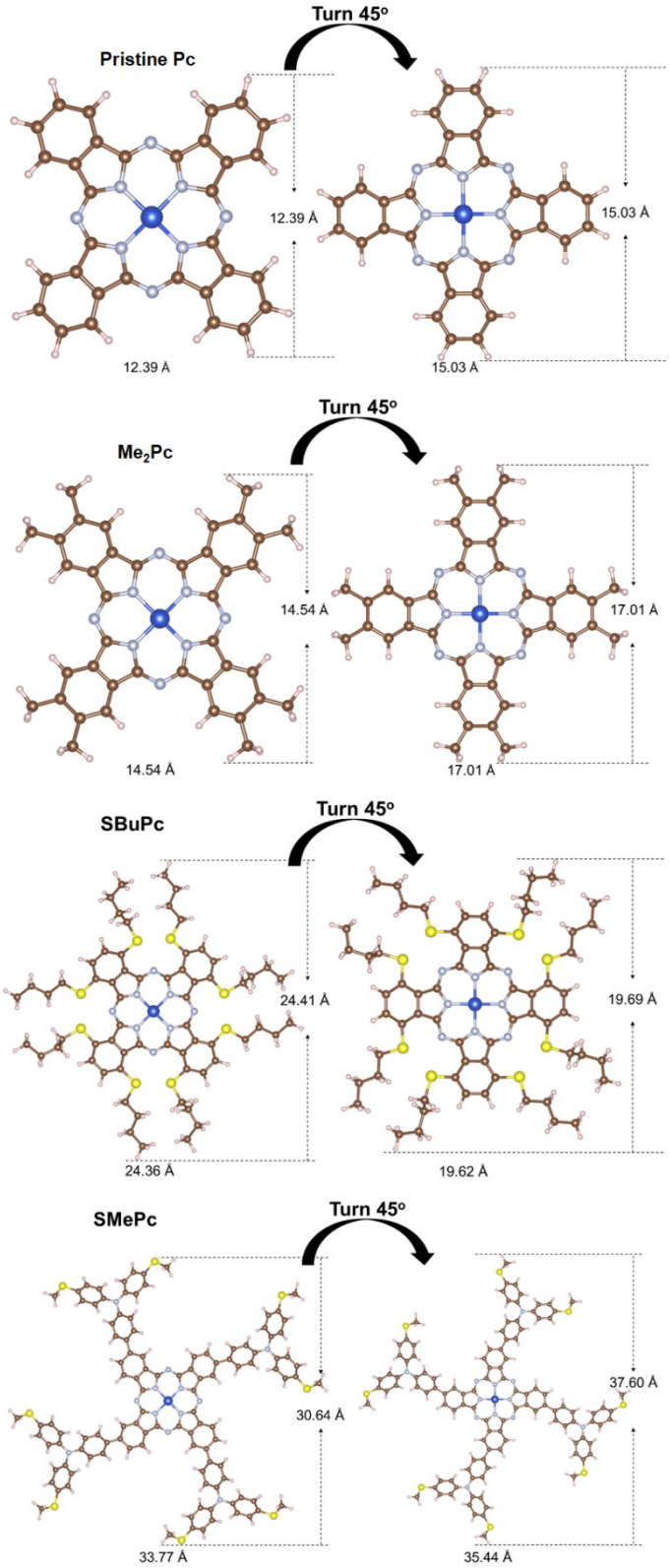

Figure S24. Molecular length parameters provided from static DFT calculation.

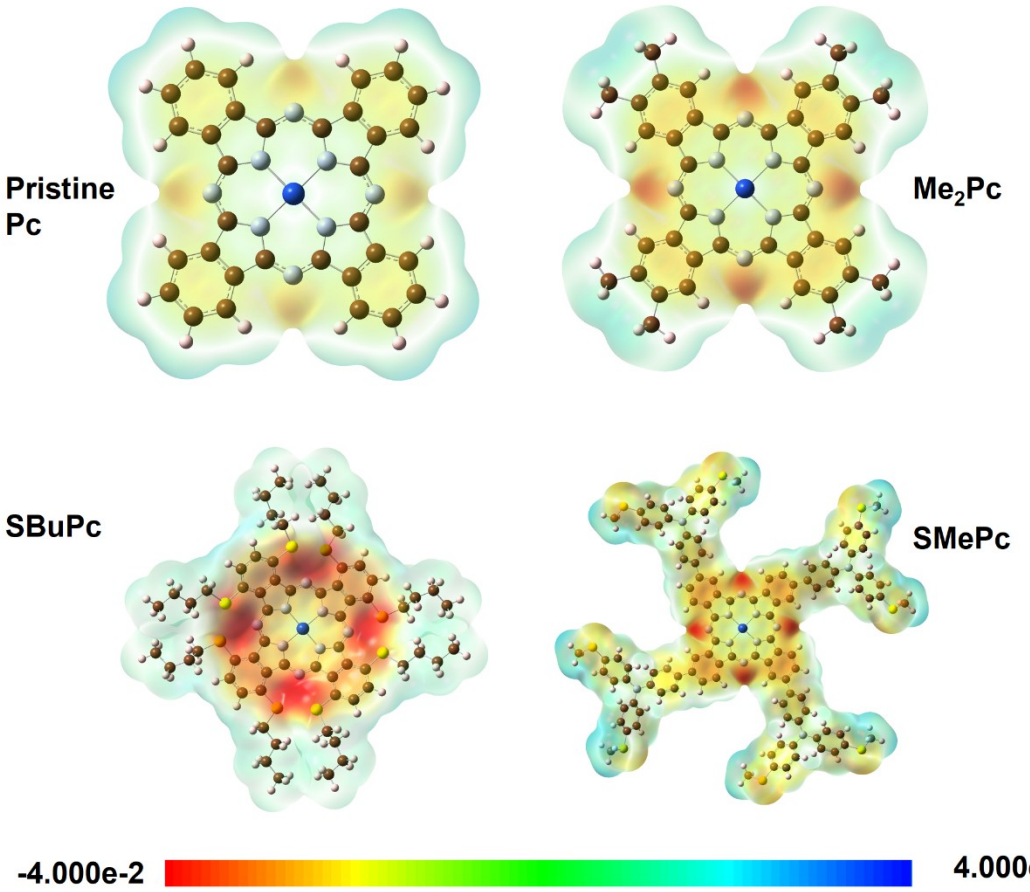

Figure S25. Electrostatic potential surface (EPS) for Pcs molecules. The blue regions represent positively charged species, while the red regions represent the negatively-charged species.

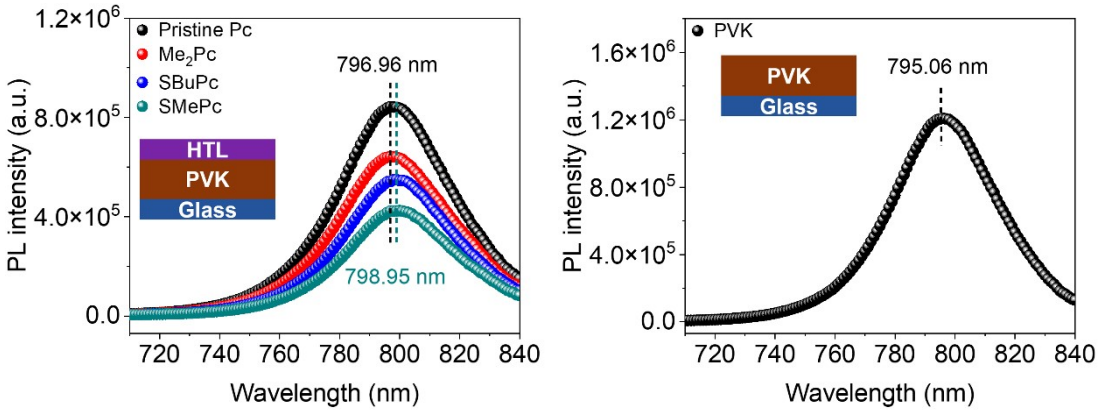

Figure S26. PL spectra for perovskite samples without HTL (Control) and with HTLs (Pristine Pc, Me_2Pc, SBuPc and SMePc).

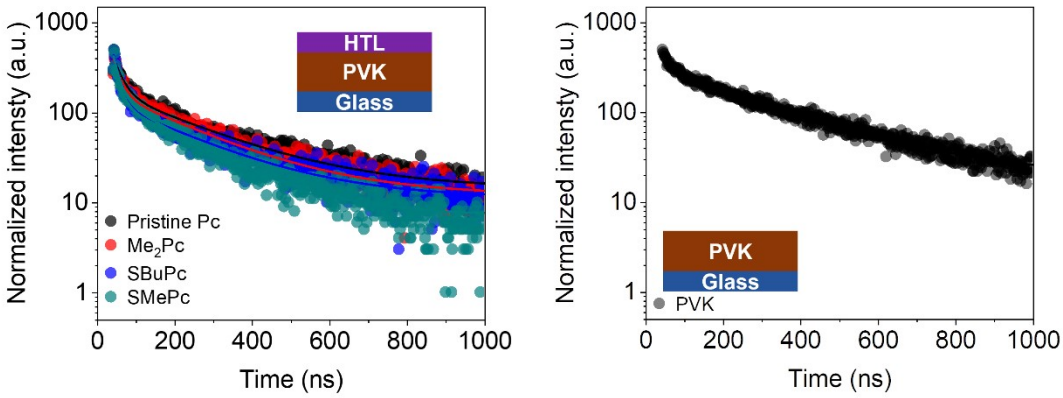

Figure S27. TRPL spectra for perovskite samples without HTL (right) and with HTLs (left).

3. Tables S1 to S10

Table S1. Fitted SEV/SRV values of MA perovskite-based samples.

Sample	SEV/SRV (cm/s)
Pristine perovskite	800 ± 400
Spiro-OMeTAD	1500 ± 200
Pristine Pc	10100 ± 2200
Me_2Pc	11200 ± 1800
SBuPc	16500 ± 1600
SMePc	19300 ± 2600

Table S2. Global fitted SEV values of FA based samples

Sample	SEV/SRV (cm/s)
Pristine perovskite	200 ± 120
Spiro-OMeTAD	2600 ± 600
Pristine Pc	11500 ± 850
Me_2Pc	12900 ± 1000
SBuPc	17600 ± 1300
SMePc	21900 ± 1500

Table S3 The SEV values of selected organic HTLs at different carrier density with MA based perovskites

Carrier Density		Surface Extraction Velocity (cm/s)			
(cm^{-3})	Spiro-OMeTAD	Pristine Pc	Me_2Pc	SBuPc	SMePc
7.5×10^{17}	1500 ± 200	10100 ± 2800	11200 ± 1100	16500 ± 1900	19300 ± 1500
1.5×10^{18}	1500 ± 200	14300 ± 2900	15300 ± 1300	22200 ± 2000	27100 ± 1900
3.0×10^{18}	1520 ± 200	18000 ± 2900	18700 ± 1500	34500 ± 2100	41700 ± 1800
6.0×10^{18}	1680 ± 200	22200 ± 2800	24400 ± 1600	43700 ± 2200	52600 ± 1700
1.2×10^{19}	2650 ± 400	29300 ± 3000	33000 ± 1600	54700 ± 2200	65200 ± 1900

Table S4 The SEV values of selected organic HTLs at different carrier density with FA based perovskites.

Carrier Density		Surface Extraction Velocity (cm/s)			
(cm^{-3})	Spiro-OMeTAD	Pristine Pc	Me_2Pc	SBuPc	SMePc
7.5×10^{17}	2600 ± 700	11500 ± 1400	12900 ± 2100	17600 ± 1700	21900 ± 2600
1.5×10^{18}	2600 ± 600	14500 ± 1500	16200 ± 2000	26100 ± 2600	33600 ± 2900
3.0×10^{18}	3300 ± 600	18400 ± 1500	21200 ± 2000	37500 ± 2500	50200 ± 2900
6.0×10^{18}	3900 ± 600	23600 ± 1400	28000 ± 1900	50700 ± 2600	62400 ± 3000
1.2×10^{19}	4400 ± 400	32300 ± 1100	36600 ± 1800	60200 ± 2600	78900 ± 3100

Table S5. Photovoltaic parameters of MA based perovskites solar cells with pristine Pc, Me_2Pc, SBuPc and SMePc.

Sample	J_{SC} (mA/cm^2)	V_{OC} (V)	FF (%)	PCE (%)
Pristine Pc	22.33 ± 0.61	0.94 ± 0.02	67.61 ± 3.02	14.63 ± 0.72
Me_2Pc	22.46 ± 0.58	0.97 ± 0.01	70.98 ± 2.46	15.74 ± 0.71
SBuPc	22.47 ± 0.46	0.98 ± 0.02	76.21 ± 2.24	17.08 ± 0.64
SMePc	22.64 ± 0.48	1.07 ± 0.01	79.79 ± 1.76	18.92 ± 0.58

Table S6. PV performance for FA-based perovskites devices.

Sample		J_{SC} (mA/cm^2)	V_{OC} (V)	FF (%)	PCE (%)	Hysteresis index
Pristine Pc	Forward	24.80	0.94	76.12	17.65	0.05
	Reverse	24.74	0.97	77.78	18.66	
Me_2Pc	Forward	24.92	0.96	76.27	18.23	0.07
	Reverse	24.95	1.00	78.71	19.60	
SBuPc	Forward	24.94	0.99	78.77	19.50	0.06
	Reverse	24.92	1.03	80.81	20.75	
SMePc	Forward	25.03	1.11	79.93	22.12	0.06
	Reverse	25.07	1.14	82.75	23.59	

Table S7. PV performance for dopant free HTM devices.

HTM	V_{OC} (V)	J_{SC} (mA/cm^2)	FF (%)	PCE (%)	Certified PCE (%)	Ref
BDT-C8-3O	1.163	25.51	81.31	24.11	23.82	*Angew. Chem. Int. Ed.*, 2023, **62**, e202312231
BTP1-2	1.178	24.95	82.83	24.34	-	*Angew. Chem. Int. Ed.*, 2023, **62**, e202218752
PMSe	1.19	25.07	82.17	24.53	-	*J. Am. Chem. Soc.*, 2022, **144**, 9500-9509
GA-P3HT	1.15	25.5	83.8	24.6	-	*Energy Environ. Sci.*, 2021, **14**, 2419
PTAA-P1	1.17	25.50	83.28	24.89	24.50	*Adv. Mater.*, 2023, **35**, 2208431
SMePc	1.163	25.10	85.45	24.95	24.43	This work

Table S8. PV

PVK	HTM	1Sun PCE (%)	Concentrated PCE (%)	Solar Concentration (Suns)	
$Cs_{0.05}(FA_{0.9}MA_{0.1})_{0.95}Pb(I_{0.9}Br_{0.1})_3$	Spiro-OMeTAD	19.4	20.3	3	J. Energy
CsMAFAPbIBr	Spiro-OMeTAD	20.5	21.1	10	ACS Appl
$(FAPbI_3)_{0.875}(MAPbBr_3)_{0.125}(CsPbI_3)_{0.1}$	Spiro-OMeTAD	21.0	21.6	1.78	Sustainal
$FA_{0.83}Cs_{0.17}PbI_{2.7}Br_{0.3}$	Spiro-OMeTAD	21.1	23.6	14.49	Nat.
$(FASnI_3)_{0.6}(MAPbI_3)_{0.4}$	PEDOT:PSS	21.18	22.36	4.17	ACS Appl
CsFAPbIBr	CuSCN	22.46	24.93	40	J Phys
$Cs_{0.04}Rb_{0.02}MA_{0.02}FA_{0.92}PbI_3$	SMePc	24.27	27.30	5.9	

Table S9. XPS data results

Sample	BE(eV)						A		
	$SOX_{1/2}$	$SOX_{3/2}$	$C\text{-}S\text{-}C_{1/2}$	$C\text{-}S\text{-}C_{3/2}$	Pb-S	$SOX_{1/2}$	$SOX_{3/2}$	C-S-C
SBuPc	169.42	167.56	164.05	162.85	\	3.0	5.9	42.
SBuPc w/ PVK	169.46	168.46	164.12	162.94	161.12	2.7	2.8	42.
SMePc	168.23	166.51	164.48	163.36	\	6.3	11.9	47.
SMePc w/ PVK	168.45	166.37	165.02	163.84	161.44	9.3	9.9	15.

Table S10. Summary of the parameters from fitting to the TRPL measurement data

Sample	A_1 (%)	τ_1 (ns)	A_2 (%)	τ_2 (ns)	τ_{Ave} (ns)
PVK	84.53	19.11	15.47	271.45	58.14
Pristine Pc	88.46	23.31	11.54	223.58	46.42
Me_2Pc	91.64	19.53	8.36	208.51	35.33
SBuPc	94.85	17.57	5.15	207.07	27.32
SMePc	95.04	16.36	4.96	165.18	23.74

Table S11. The adsorption energies of pristine Pc, Me_2Pc, SBuPc, and SMePc on the perovskite surface. The adsorption energy (E_{ads}) is obtained from $E_{ads}=E_{Pcs/PVK} - E_{Pcs} - E_{PVK}$, where $E_{Pcs/PVK}$ represents the energy of adsorbed configuration, while the E_{Pcs} and E_{PVK} are the energies of the Pcs molecule and the perovskite, respectively.

Molecule	Total energy (au)	Perovskite energy (au)	Molecular energy (au)	Adsorption energy(au)	Adsorption energy(eV)
Pristine Pc	-7516.35	-7196.88	-318.96	-0.51	-13.84
Me_2Pc	-7571.44	-7196.88	-374.01	-0.55	-15.04
SBuPc	-7818.03	-7196.88	-620.55	-0.605	-16.47
SMePc	-8132.94	-7196.88	-935.37	-0.69	-18.78

4. References:

S1 Qu, G. *et al.* Dopant-Free Phthalocyanine Hole Conductor with Thermal-Induced Holistic Passivation for Stable Perovskite Solar Cells with 23% Efficiency. *Adv. Funct. Mater.* **32**, 2206585, (2022).

S2 Yang, G. *et al.* A facile molecularly engineered copper (II) phthalocyanine as hole transport material for planar perovskite solar cells with enhanced performance and stability. *Nano Energy* **31**, 322-330, (2017).

S3 Hu, Q. *et al.* Dual Defect-Passivation Using Phthalocyanine for Enhanced Efficiency and Stability of Perovskite Solar Cells. *Small* **17**, 2005216, (2021).

S4 Yang, Y. *et al.* Top and bottom surfaces limit carrier lifetime in lead iodide perovskite films. *Nat. Energy* **2**, 16207, (2017).

S5 Xue, J. *et al.* Reconfiguring the band-edge states of photovoltaic perovskites by conjugated organic cations. *Science* **371**, 636, (2021).